OPTIMIZED RADIATION DOSE AND IMAGE QUALITY FOR ABDOMINAL CT PROTOCOL: PHANTOM STUDY

SAIMAI SIANGYAI

A THESIS SUBMITTED IN PARTIAL FULFILLMENT
OF THE REQUIREMENTS FOR
THE DEGREE OF MASTER OF SCIENCE
(RADIOLOGICAL SCIENCE)
FACULTY OF GRADUATE STUDIES
MAHIDOL UNIVERSITY
2018

Thesis
entitled

OPTIMIZED RADIATION DOSE AND IMAGE QUALITY FOR ABDOMINAL CT PROTOCOL: PHANTOM STUDY

.....

Ms. Saimai Siangyai
Candidate

.....

Assoc. Prof. Malulee Tuntawiroon,
M.Sc. (Medical Physics), M.Sc. (Nuclear Medicine)
Major advisor

.....

Assoc. Prof. Dittapong Songsaeng,
M.D.
Co-advisor

.....

Prof. Patcharee Lertrit,
M.D., Ph.D. (Biochemistry)
Dean
Faculty of Graduate Studies
Mahidol University

.....

Assoc. Prof. Malulee Tuntawiroon,
M.Sc. (Medical Physics), M.Sc. (Nuclear Medicine)
Program Director
Master of Science Program in Radiological Science
Faculty of Medicine Siriraj Hospital
Mahidol University

Thesis
entitled

OPTIMIZED RADIATION DOSE AND IMAGE QUALITY FOR ABDOMINAL CT PROTOCOL: PHANTOM STUDY

was submitted to the Faculty of Graduate Studies, Mahidol University
for the degree of Master of Science (Radiological Science)
on
January 5, 2018

.....
Ms. Saimai Siangyai
Candidate

.....
Asst Prof. Phensri Sirikunakorn,
M.D, M.Sc. (General Radiology)
Chair

.....
Assoc. Prof. Nopamon Sritongkul,
M.Sc. (Biochem)
Member

.....
Assoc. Prof. Malulee Tuntawiroon,
M.Sc. (Medical Physics), M.Sc. (Nuclear Medicine)
Member

.....
Prof. Patcharee Lertrit,
M.D., Ph.D. (Biochemistry)
Dean
Faculty of Graduate Studies
Mahidol University

.....
Prof. Prasit Watanapa,
M.D., Ph.D., FRCS, FACS
Dean
Faculty of Medicine Siriraj Hospital
Mahidol University

ACKNOWLEDGEMENTS

I would like to express my sincere appreciation to those whose cooperation and assistance made this thesis complete. Many people supported me in preparing this thesis, and their help is gratefully acknowledged. I would like to express my special appreciation to my advisor, Associate Professor Malulee Tuntawiroon for her guidance, encouragement and continuous support throughout the thesis work.

I would like to thank Associate Professor Dr. Dittapong Songsaeng, Ms. Supawan Jivapong, Assistant Professor Pacharin Prapaisilp and all staff members of Siriraj Imaging Center for their useful advice, helpful support and co-operation to accomplish this thesis.

I am indebted to Head of the Department of Radiology, my colleagues at the Section of Diagnostic Radiology as well as all administrative staff members of the Faculty of Medicine Vajira Hospital, Navamindradhiraj University, for allowing me time off for continuing my education.

My thanks are also extended to all my friends for their several valuable suggestions.

Finally, this work is dedicated to family members for their love and encouragement during the past years.

Saimai Siangyai

OPTIMIZED RADIATION DOSE AND IMAGE QUALITY FOR ABDOMEN CT PROTOCOL: PHANTOM STUDY

SAIMAI SIANGYAI 5638168 SIRS/M

M.Sc. (RADIOLOGICAL SCIENCE)

THESIS ADVISORY COMMITTEE: MALULEE TUNTAWIROON, M.Sc. (MEDICAL PHYSICS), M.Sc. (NUCLEAR MEDICINE), DITTAPONG SONGSAENG, M.D.

ABSTRACT

This study aims to determine the appropriate radiation dose to achieve an acceptable image quality of an abdominal body phantom when varying the Noise Index in the routine abdominal CT scan protocol at Siriraj Diagnostic Imaging Center, using 2 CT systems, GE Medical System, Model VCT Light Speed and Model HD750. The radiation Noise Index of CT images was measured on standard, large and very large size phantoms. Radiation doses were recorded using fix mode (500 mA) and auto modulation (Noise Index 0 – 20), and the image quality was evaluated by measuring the noise in the image of five regions of interest ; Right Liver lobe, Left Liver lobe, Spleen, Aorta and Left kidney.

By varying the Noise Index from 0–20 at slice thicknesses of 1.25 and 7.0 mm on the standard, large and very large size phantoms, the estimated radiation doses increase with body size : 4.57, 5.36 and 6.44 mSv for standard, large and very large body size, respectively. The image noise was higher for the thin slices (1.25 mm) than for the thick slices (7 mm). An image quality can be enhanced by Noise Index reduction in the process of image reconstruction using adaptive statistical iterative reconstruction and Model-Based iterative reconstruction software.

It can therefore be concluded that factors affecting radiation dose and image quality were Noise Index, slice thickness and reconstruction method. A greater radiation dose is required for larger patients, or to decrease the Noise Index. Thin slices yielded poorer image quality than did thick slices, but showed details more clearly. The results obtained from this study can be used to make small changes in the selection of an appropriate image processing method for abdominal CT scans which can reduce the dose of radiation used while still providing the required clinical information.

KEY WORDS: CT PROTOCOL/ BODY PHANTOM/ NOISE INDEX

49 pages

การปรับปริมาณรังสีอย่างเหมาะสมเพื่อให้เกิดภาพที่มีคุณภาพยอมรับได้สำหรับโปรโตรคอลการตรวจเอกซเรย์คอมพิวเตอร์ช่องท้อง: ศึกษาในหุ่นจำลอง
OPTIMIZED RADIATION DOSE AND IMAGE QUALITY FOR ABDOMEN CT PROTOCOL: PHANTOM STUDY

สายใหม เสียงใหญ่ 5638168 SIRS/M

วท.ม.(วิทยาศาสตร์รังสี)

คณะกรรมการที่ปรึกษาวิทยานิพนธ์: มลุลี ตัณฑวิรุฬห์,วท.ม.(ฟิสิกส์การแพทย์), วท.ม.(เวชศาสตร์นิวเคลียร์), ฑิตพงษ์ ส่งแสง, พ.บ., ป.ชั้นสูง (รังสีวิทยา), ว.ว. (รังสีวิทยาทั่วไป), อ.ว. (เวชศาสตร์ครอบครัว)

บทคัดย่อ

การศึกษาครั้งนี้มีจุดมุ่งหมายเพื่อหาปริมาณรังสีที่เหมาะสมเพื่อให้ได้ภาพที่ได้รับการยอมรับในระดับที่ยอมรับได้สำหรับโปรโตคอลการตรวจเอกซเรย์คอมพิวเตอร์ช่องท้อง : ศึกษาในหุ่นจำลอง ณ ศูนย์ภาพวินิจฉัยโรงพยาบาลศิริราชโดยใช้ เครื่องเอกซเรย์คอมพิวเตอร์ชนิด 64 หัววัดของบริษัท GE (General Electric Medical System) รุ่น Light Speed VCT และ รุ่น Discovery CT750 HD โดยฉายลำแสงเอกซ์ผ่านหุ่นจำลองที่ต้องการศึกษาและให้คอมพิวเตอร์สร้างภาพในแนวตัดขวาง ภาพที่ได้จึงเป็นภาพตัดขวางของหุ่นจำลองที่ต้องการศึกษาอย่างละเอียด โดยวัดได้จากหุ่นจำลองที่ขนาดปกติ ขนาดใหญ่และขนาดใหญ่มาก โดยใช้โหมดคงที่ในการสร้างภาพ ที่ 500 mA และ Noise Index 0 - 20 ได้บันทึกปริมาณรังสีและตรวจสอบคุณภาพของภาพด้วยการวัดพื้นที่ที่สนใจ 5 ตำแหน่งได้แก่ กลีบตับด้านขวา, กลีบตับด้านซ้าย, ม้าม, เส้นเลือดแดง,ไตข้างซ้ายจากการเปลี่ยนแปลงค่าดัชนีนอยส์จาก 0-20 ที่ความหนา 1.25 และ 7.0 มิลลิเมตรในหุ่นจำลองขนาดมาตรฐานขนาดใหญ่และขนาดใหญ่มาก พบว่าปริมาณรังสีเพิ่มขึ้นตามขนาดของหุ่นจำลอง สำหรับภาพที่ความหนา 1.25 มิลลิเมตรค่าดัชนีนอยส์สูงกว่าภาพที่ความหนา 7 มิลลิเมตร คุณภาพของภาพสามารถเพิ่มขึ้นได้โดยการลดค่าดัชนีนอยส์ การสร้างภาพด้วย MBIR แสดงให้เห็นถึงศักยภาพที่ดีในการลดปริมาณรังสีที่ตรวจบริเวณช่องท้องใน CT ได้ร้อยละ 70-90 ส่วน ASIR จะถูกจำกัดในเรื่องนี้เนื่องจากคุณภาพของภาพที่ลดลง ปริมาณรังสีจะเพิ่มขึ้นตามขนาดมาตรฐานขนาดใหญ่และขนาดใหญ่มากคือ 4.57, 5.36 และ 6.44 ค่า $CTDL_{vol}$ ที่ได้ถูกบันทึกจากหน้าจอแสดงภาพสรุปได้ว่าปัจจัยที่มีผลต่อปริมาณรังสีและคุณภาพของภาพ ได้แก่ ค่าดัชนีนอยส์ความหนาของหุ่นจำลอง การเพิ่มค่าดัชนีนอยส์และการเพิ่มขนาดของหุ่นจำลอง จะเพิ่มปริมาณรังสี ความหนาของหุ่นจำลองขนาดบางให้คุณภาพของภาพต่ำกว่าชิ้นหนา แต่ให้รายละเอียดที่ดีขึ้น ใช้ผลเพื่อปรับเปลี่ยนโปรโตคอลที่ใช้ในกระบวนการ CT บนช่องท้องและลดปริมาณรังสีให้กับผู้ป่วย

49 หน้า

CONTENTS

LIST OF TABLES

LIST OF TABLES (cont.)

LIST OF FIGURES

LIST OF FIGURES (cont.)

LIST OF FIGURES (cont.)

LIST OF ABBREVIATIONS

Abbreviations	Term
CT	Computed tomography
AAPM	The American Association of Physicists in Medicine
kVp	Kilovoltage peak
mA	milli Ampere
mAs	milli Ampere sec
AEC	Automatic exposure control
SD	Standard deviation
FBP	Filtered back projection
ROI	regions of interest
SNR	Signal-to-noise ratio
CNR	Contrast-to-noise ratio
ASIR	Adaptive Statistical Iterative Reconstruction
MBIR	Model-Based Iterative Reconstruction
MDCT	Multi Detector Computed Tomography
HDCT	High Dose Computed Tomograph

CHAPTER I
INTRODUCTION

Current imaging technology in medical diagnosis is developed very quickly. The examination with X-ray computer (CT scan) is to detect abnormalities of various organs in the body with the X-ray beam. The projection beam output through an organ producing cross-sectional image of specific area of a scan object. The images generated were in the axial or transverse planes, perpendicular to the long axis of the body. Use of CT has increased dramatically for over more than two decades in many countries.

Diagnostic Radiology Imaging Center at Siriraj Hospital performs a wide range of procedures with varieties of x-ray computed tomography (CT) from different CT scanner manufacturers. Different version of CT scanners may show different detail or sharpness of the image according to the selected protocol and image processing method on each scanner. An instruction protocol which varies according to organ to be investigated as well as shape and size of the patient can be selected to suit different version of CT scanners. Appropriate setting for patient dose reduction can be adjusted to obtain the best image quality for clinical diagnosis.

The purpose of this study is to determine appropriate parameters to standardize and optimize the CT protocols to achieve low dose in diagnostic CT examination of upper abdomen using 2 GE CT scanners, 64 slice LightSpeed VCT, and 64 slice Discovery CT750 HD. Human body anthropomorphic phantom of standard, large and very large sizes are used to demonstrate effects of changing technical factors. Image quality and radiation dose quantities from the 2 scanners are to be compared. Abdominal scan is selected for the study because it is a common procedure performed, in some patients, long-term CT scan follow-up was conducted for several years. Therefore, some program modification and technical parameters adjustment should be applied to reduce radiation exposure while maintaining image quality and clinical information.

CHAPTER II
OBJECTIVES

2.1 General objective

2.1.1 To determine the radiation dose from standard protocols for CT scan of upper abdomen in achieving an acceptable image quality. Due to some limitations on patient dose measurements, anthropomorphic phantoms have been used for this study.

2.1.2 To compare image quality and radiation dose quantities between two scanners when routine upper abdomen protocol is used.

2.1.3 To study technical factors affecting image quality and dose quantities of the routine upper abdomen protocol with anthropomorphic phantoms.

2.2 Specific objective

To compare radiation dose and image quality between 2 different GE scanners using standard settings for different image reconstruction methods in anthropomorphic phantom of standard, large and very large sizes to simulate the average adult patients and patients with different body sizes.

CHAPTER III
LITERATURE REVIEWS

3.1 Background and rationale

Computed Tomography (CT)

Computed tomography (CT) scanners also known as computerized axial tomography (CAT) scanning, have been available since the mid-1970s and have revolutionized medical imaging. CT scan is a diagnostic imaging procedure that uses X-rays to build cross-sectional or tomographic images of the body. A tomographic image is an image of a slice through the body. This imaging technique is applied to obtain anatomical images of all parts of the human body. Compared to the projection images in conventional X-ray photography, the slice images give a much better contrast between different tissues. This is one of the main advantages of CT. Today, millions of scans are performed worldwide every year solving different clinical questions in a variety of clinical fields. CT is also widely used in emergencies as it the rapid and most accurate tools in delivers detailed information, which is essential for appropriate treatment decisions[1] .

CT scans are valuable in emergencies because they can provide clinical information very quickly especially when assessing strokes, brain injuries, heart disease, and internal injuries. The short duration of the scanning process benefits patients who are not easily able to keep still, such as children[2] . CT imaging is a very important tool to diagnose cancer and to obtain additional information for different clinical questions. A CT scan usually requires a higher radiation exposure dose than a conventional radiography examination. Radiation doses in CT are relatively high. The effective dose of a head scan is approximately 2 mSv, of the thorax 10 mSv and of the abdomen may be as high as 15 mSv[3].

Although the radiation dose is higher than radiographic images of the same region, the diagnostic content of the CT images is typically much higher. Some scanners use a lower tube current and a higher voltage to reduce the dose. However,

there is still some risk to a developing foetus. CT scans are therefore not recommended during pregnancy unless the examination is absolutely necessary. Doctors and manufacturers do all they can to minimize radiation dose.

Principles of CT scan and Image Reconstruction

Computed tomography is an imaging technique that produces cross-sectional images, representing in each pixel the local X-ray attenuation properties of the body. CT scanner has been continuously modified and improved since its introduction. It has undergone several changes with increase in number of detectors and decrease in the scan time. The important elements of CT scanner are x-ray tube and detector array, which are mounted on rotating circular system, allows scanning and obtaining information about the scanned body from every angle. Principle of CT scan is shown in Fig. 3.1[4] , a thin collimated beam of X-rays passes through the body to a detector that measures the transmitted intensity. The collimator is a set of narrow lead tubes or an array of small holes in a lead plate, resulting in a thin straight beam of X-rays.

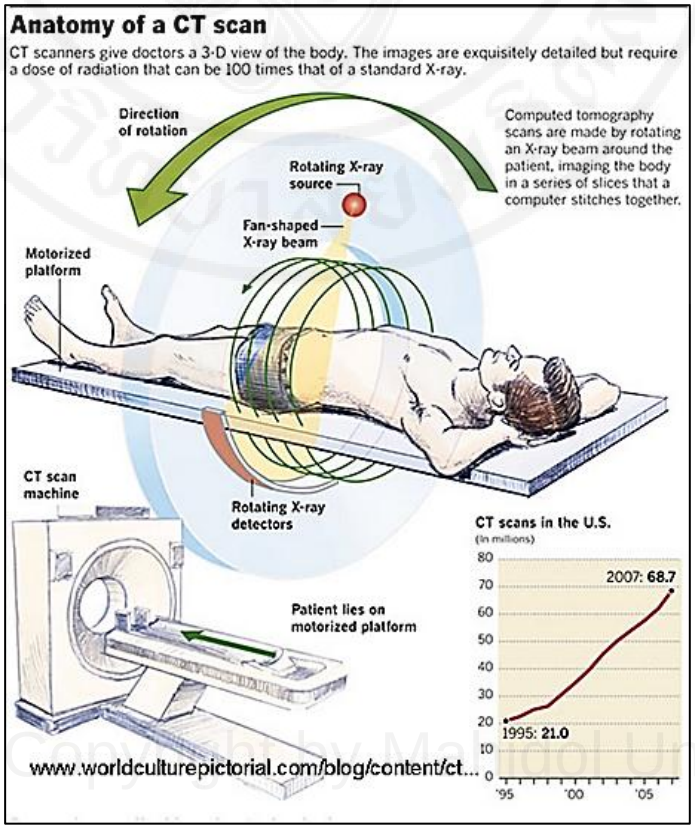

Figure 3.1 Principles of CT scan.

Based on the fundamental principle that the density of the tissue passed by the X-ray beam can be measured from the calculation of the attenuation coefficient, data for the final image is obtained by measuring attenuation of radiation on the path from X-ray tube, which generates the X-rays, through the object, to the detector. CT allows the reconstruction of the density of the body, by two-dimensional section perpendicular to the axis of the acquisition system. Attenuation may cause by absorption or by scattering of photon from the beam, basically by the two processes, photoelectric and Compton effects. The equation $I = I_o\, e^{-\mu x}$ expresses the exponential relationship between incident primary photons and transmitted photons for a monoenergetic beam with respect to the thickness of the absorber. Where I_o and I represent the intensity of the x-ray beam before and after passing through substance, x is the thickness of the material and μ is defined as the linear attenuation coefficient.

The attenuation profile obtained this way is not a universal value, generally, the linear attenuation coefficient is normalized to that of a standard material, such as water, and is defined as the CT numbers of the materials. To honour Hounsfield for his work the mean X-ray attenuation within one pixel or CT number is expressed in Hounsfield units (HU). Measured values of attenuation are transformed into CT numbers using the international Hounsfield scale as shown in the following equation.

$$\boldsymbol{CT\ Number} = \frac{(\boldsymbol{\mu_{tissue}} - \boldsymbol{\mu_{water}})}{\boldsymbol{\mu_{water}}}\mathbf{1000}$$

The number 1000 are referred to as the Hounsfield (H) Scale, μ_{tissue} is the linear attenuation coefficient of the tissue of interest, and μ_{water} is the linear attenuation coefficient of water. In computed tomography, the CT numbers or the Hounsfield scale of tissue density is established on a relative basis with the attenuation of water as a reference. On the H scale, CT number for water is always 0 and those for bone and air are +1000 and – 1000 (minimum HU value) respectively. Density of other tissues is related to this range, usually from -1000 to +1000HU.

CT Image Quality

Components of image quality are noise, slice thickness or Z-axis resolution, low contrast resolution and high contrast resolution.

Image Noise

Image noise is random uncertainties in CT number. The random noise in a CT image limits the ability of the observer to discriminate between two regions of different density. It is unpredictable and cannot be completely eliminated from the image and this will lead to uncertainty in the interpretation of the image. Reduction in the magnitude of image noise can lead to an improvement of the detection of contrast differences. It is measured as the standard deviation of voxel values in a water phantom. These variations in pixel intensities have random and systematic components. Image noise is an important factor in determining dose to the patient. The very important issue of optimizing a CT imaging protocol involves producing a balance among image detail, image noise, and the dose to the patient.

Much more complete definitions of noise that take into account the contrast scale of the scanner was described in AAPM report No. 39[5] . Image noise is influenced by a large number of parameters, including:

(1) Tube voltage (kVp)
(2) Slice thickness
(3) Tube current (mA)
(4) Exposure time
(5) Reconstruction algorithm or filter
(6) Helical Pitch/Table speed
(7) Others (Focal spot to isocenter distance, detector efficiency, etc.)

Slice Thickness

The reconstructed slice thickness of an image has become much more interesting and complex when going from axial scanning to helical scanning and to multidetector helical scanning. In this study, we will focus only on the reconstructed slice width in helical scanning and the factors that may influence it, these include:

(1) Noise index
(2) Phantom size
(3) Detector width
(4) Reconstruction technique

Radiation Dose

Radiation dose is related to the amount of energy that x-ray photons deliver during a CT scan. The total number of photons is proportional to the tube current (mA) and the X-ray beam on time in seconds during a single rotation of the gantry. This is proportional to the tube current–time product (mAs). Advances CT technology in recent years allowed high-quality examinations to be performed at lower radiation dose. There are many possible strategies to reduce radiation exposure from CT scan while maintaining acceptable diagnostic image quality for clinical information. The radiation dose measured in phantoms by a particular imaging protocol as described by $CTDI_{vol}$. Technical factors which influenced radiation exposure from CT scan include:

(1) kVp
(2) mA
(3) Exposure tome
(4) X-ray Beam collimation
(5) Pitch (Table Speed)
(6) Effects of Algorithm and Collimation
(7) Dose Reduction Options (such as tube current modulation techniques)

Several of these parameters have been described as possible mechanisms to reduced radiation dose to patients[6]. These included recommendations to:

(1) Reduce tube current (mA)
(2) Increase table increment (axial) or pitch
(3) mA settings based on patient weight (or diameter) and body region
(4) Reduce number of multiple scans w/contrast
(5) Eliminate inappropriate referrals for CT

Tradeoffs between Radiation Dose and Image Quality

As parameters are varied to reduce radiation dose, the impacts on image quality must be considered as there are often direct tradeoffs between these two parameters. Some examples of tradeoffs include:

Reduction of mAs

The relationship between tube current and patient dose is linear. For a single axial scan radiation dose is directly proportional to the tube current–time product. Increases in tube current (mA) or the product of tube current and scan time (mAs) results in improved image quality, decreased image noise, and increased patient dose. Increases in mAs resulting in a comparable percentage increase in patient dose. Although tube current can be manually controlled, most operators use automated tube current modulation (AEC) for most applications. Radiation dose reduces in proportion to reduction in mAs, but increases image noise proportionally. For example, if the mAs is reduced to ½ of the original, the noise is expected to increase by 1.41 (41% increase)[7]. The low contrast resolution performance of the CT image will be degraded.

Increase table speed or pitch

The relationship between table increment per rotation and slice thickness or collimator width is referred to as pitch[8]. The absorbed dose in CT scan is dependent on pitch. Pitch is a fundamental parameter in helical scan modes which is defined as table travel per rotation divided by beam collimation. Pitch plays an important role in absorbed dose, image quality and scan time. A smaller pitch increased overlap of anatomy and increased sampling at each location, results in an increased radiation dose. A low-pitch technique is associated with less image noise, and improved signal-to-noise and contrast-to-noise ratios. Alternatively, a larger pitch increased gaps in the anatomy results in lower radiation dose. Increasing pitch linearly reduces radiation dose but there will be a lack of data collection between each slice which can cause inaccuracies in the image reconstruction process leading to artifacts in the scan image[9].

Reducing kVp

Radiation dose depends on the total number of photons and their individual energies. The energy distribution of these photons depends on the x-ray tube potential (kVp) and the filter. Radiation dose changes with the square of kVp. Reducing kVp can be an effective means of reducing the radiation dose imparted during an examination. When iodine is used as vascular contrast particularly in angiographic studies, reductions in kVp increased attenuation of iodine as a result of the photoelectric effect. At the k-absorption edge of iodine, contrast-to-noise ratios are potentially improved[10].

It is now widely accepted that low-kVp protocols (even 70 kVp) are most useful particularly in vascular or angiographic studies in thin, non-obese patients, in which improvements in the attenuation of iodine can be helpful in terms of image contrast-to-noise ratios[11]. However, too low kVp technique can result in nonlinear, exponential increases in image noise. To compensate for increase in noise, increase in mAs is used to preserve image quality, which in turn will increase radiation dose. The use of low kVp in a number of different protocols with iodine contrast have shown that kVp reductions can markedly reduce radiation doses, while still preserving acceptable image quality.

3.2 Review of Related Literature

Pawana Inthibal[12] , et al conducted a phantom study on Optimization in 64-MDCT of the chest using tube current modulation based on noise index with the purpose to determine the radiation dose when varying Noise Index and the optimal Noise Index for the acceptable image quality of the chest phantom. By varying Noise Index between 10-20 and the slice thickness between 0.625 – 5.0 mm on the standard size phantom, the radiation dose decreased, $CTDI_{vol}$ reduced from 16.52 to 3.38 mGy. The $CTDI_{vol}$ and DLP slightly decreased at the thin slice thickness and rapidly decreased at thick slice thickness on varying Noise Index. There were no variation of $CTDI_{vol}$ and DLP at the thin slice thickness for the large size phantom, the $CTDI_{vol}$ ranged from 16.52-7.09 mGy. The STD filter offered the highest percent CNR when

compared to the CHEST filter at 50-60%, the LUNG and BONE+ offered the lowest percent CNR respectively. The LUNG filter produced the best spatial resolution image. The scoring on image quality by two observers for standard, and large size phantoms were similar with good agreement. Noise Index and slice thickness are the major parameters affecting the radiation dose. Increasing Noise Index from 10 to 20 results in decreasing radiation dose to 18.2, 32.1, 64.9, and 65.9% for slice thickness of 0.625-5.0 mm respectively. The slice thickness had a major impact on radiation dose for the large size phantom with the reduction from 12.82% to 57.07 % for slice thickness of 2.5-5.0 mm respectively. The STD filters were designed for good spatial resolution with reasonably low image noise. The Noise Index has little affected on CNR. When varying Noise Index from 10 to 20, the reduction in $CTDI_{vol}$ was 16.52 and 3.38 mGy for standard size phantom, and 16.52 and 7.09 mGy for large size phantom. The factors affecting radiation dose and image quality were Noise Index, slice thickness and reconstruction filters. The selection on Noise Index depends on clinical applications. Using the Noise Index of 20 at 75-380 mA with Lung and Bone+ filters resulted in acceptable subjective image quality whereas Noise Index 15-17.5 at 75-380 mA with STD filters resulted in acceptable objective image quality for routine chest CT.

In 2012 Angjelina Protik[13] has conducted a research on the Optimization of Image Quality in Computed Tomography for Pediatrics using Catphan® 600 phantom to simulate child's body with the purpose to evaluate the GE Discovery™ CT750 HD system image quality parameters with ASIR™ and different collimation. The effects of the reconstruction program ASIR™ (Adaptive Statistical Iterative Reconstruction) on image quality parameters and potential dose reduction in pediatric CT were described. It was concluded that the images reconstructed with 50% ASIR™ demonstrated significant improvements in uniformity, noise and CNR. The results confirm that 50%ASIR™ could be used as optimal blend for body CT protocols in paediatrics.

In 2014 Eric C. Ehman et al[14] reviewed in their article, the methods for noise reduction techniques for low-dose abdominopelvic CT, including analytic reconstruction, projection and image space denoising, and iterative reconstruction; and

had discussed the strengths and limitations of individual noise reduction techniques. In phantom studies, they demonstrated that the imaging of phantoms, iterative reconstruction and nonlinear denoising may maintain high-con¬trast spatial resolution while simultaneously reduc¬ing image noise. Potential dose reduction using noise reduction methods is dependent on lesion-to-background contrast and the anatomy of interest. High-contrast tasks such as CT colonography, renal stone detection, and CT enterography will permit large reductions in radiation dose. Low-contrast tasks such as the detection of liver metastasis will permit smaller reductions in radiation dose.

In 2016 Chatnapa Nuntue[15] has conducted research on the optimization of a low-dose 320-slice multi-detector computed tomography chest protocol using a phantom with an objective to optimize a protocol for multi-detector computed tomography (MDCT) of the chest with pulmonary nodules based on targeted standard deviation (SD) to achieve minimal patient radiation exposure, while maintaining acceptable diagnostic information. At varying diameters of simulated lung nodules, CT scan was performed on a 320-slice MDCT by varying targeted SD of 9, 14, 20, and 25, beam pitch of 0.637, 0.813, and 1.388, at 120 and 100 kVp, and 10-400 mA. The radiation doses were measured in terms of $CTDI_{vol}$, quantitative image quality was determined by the percent contrast-to-noise ratio (%CNR). Detection acceptability of the CT images was evaluated by two independent radiologists. They demonstrated that increased targeted SD results in decreased radiation dose and %CNR. The reduction in $CTDI_{vol}$ was between –40% and –88% compared with the default setting for various targeted SD, beam pitch, and beam quality (kVp). At targeted SD of 9, the %CNR was highest. A good agreement (k = 0.66) between the image quality scores was observed. In conclusion, targeted SD of 20, 10-400 mA at pitch 0.813 and 120 kVp on a nodule size of 5 mm was considered the optimal protocol for low-dose chest CT.

CHAPTER IV
MATERIALS AND METHODS

This experimental study is aimed to investigate the lowest radiation dose for maintaining good image quality in upper abdomen CT scan, the most common procedures performed in most of the radiology departments, with routine protocol. The patient was simulated by human adult anthropomorphic phantom. The study was carried out using 2 GE CT scanners operating at the Diagnostic Imaging Center, Department of Radiology, and Faculty of Medicine Siriraj Hospital.

Materials and Methods

4.1 Material

4.1.1 Scanner 1: The 64 Mutidetector CT GE Medical System, Model VCT lightspeed (MDCT) (Figure 4.1), with software for noise reductions and improve image quality: Filtered back projection (FBP).

4.1.2 Scanner 2: The 64 Mutidetector CT GE Medical System, Model Discovery 750HD (HDCT) (Figure 4.2), with software for noise reduction and improve image quality: GE*'s model based iterative reconstruction (MBIR) technology or Veo*, Adaptive Statistical Iterative Reconstruction (ASIR).

4.1.3 Whole Body anthropomorphic Phantom (PBU-50; Kyoto Kagaku Co. Ltd, Japan); life-size human phantom with a life-size synthetic skeleton embedded in radiological soft tissue substitute, human tissue substitute select only thoracoabdominal part, embedded organs: lungs with vessels, mediasternal space, liver, kidney and pelvic girdle (Figure 4.3)

4.1.4 CT bismuth shielding for increasing phantom size from standard size to large and very large size.

Figure 4.1 GE 64 slice LightSpeed VCT CT Scanner.

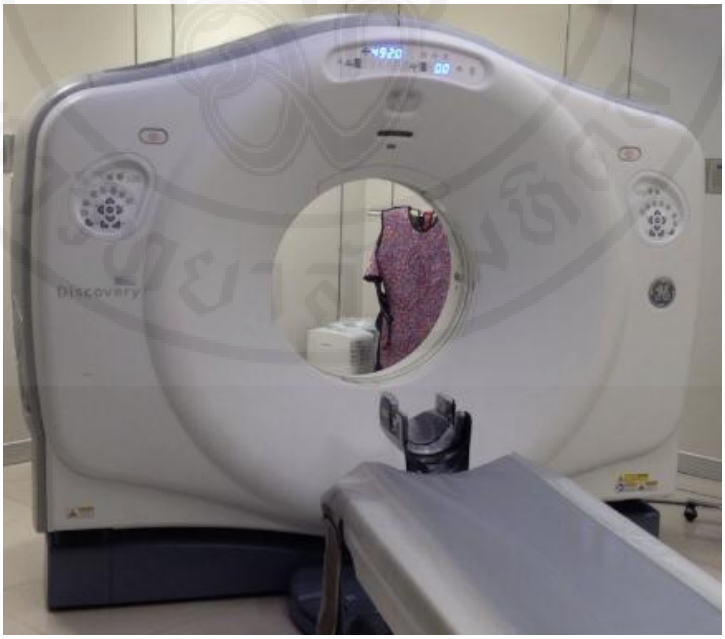

Figure 4.2 GE 64 Slice Discovery HD 750 CT Scanner.

Figure 4.3 Anthropomorphic phantom (body phantom), thoracoabdominal part, embedded organs: lungs with vessels, mediasternal space, liver, kidney and pelvic girdle.

4.2 Methods

4.2.1 Body phantom

Three different size anthropomorphic phantoms, standard (std), large (l) and very large or overlarge (ol) (Figure 4.4) were scanned using same vertical centering and were assessed with radiation dose–monitoring software. The effect of vertical positioning on the radiation dose was studied using the volume CT dose index ($CTDI_{vol}$), dose-length product (DLP), and size-specific dose estimates for different-sized phantoms. Image noise was determined from CT number histograms. The body phantom is positioned vertically for abdomen scan. The scan range was set for abdominal examination and the AEC was used to modulate tube current according to patient size and x-ray attenuation in tissues.

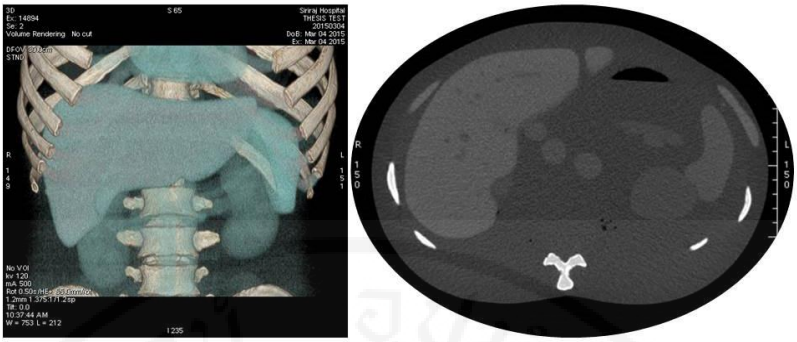

Standard size

Large size

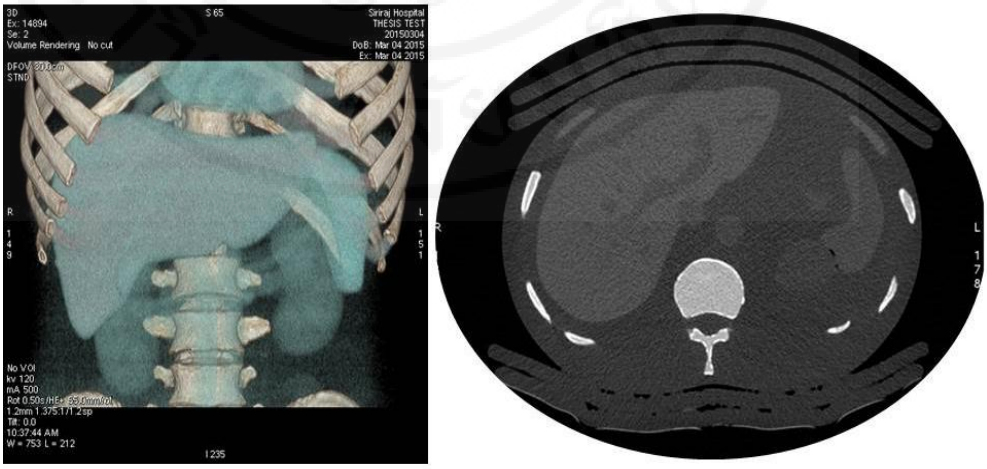

Very large size

Figure 4.4 Show 3 sizes of phantom representing standard, large, and very large size patient.

4.2.2 Scan parameter

Fix scan parameter routine protocol for Abdominal CT scan was used for all changed in scan parameters as in 4.2.3

Position	supine, orientation: feet first
	Scan helical, scannogram and axial
Scan length	dome of diaphragm to iliac crest, Landmark “0”
	at xyphoid process
Rotation time	0.5 second
kVp	120
mA	500
DFOV	32 cm
Slice thickness	1.25 mm

4.2.3 Changed in scan parameter for comparative studies

Noise index (NI)	0, 10, 15 and 20 for both two GE scanners
mA	Fix mA and Auto mA
Algorithms: MDCT	FBP
Algorithms: HDCT	ASIR 30%, 40%, 50% and MBIR 0%

4.2.4 For noise measurements, two images from each scanner were selected at 2 levels to clearly demonstrate 5 volume tissues as shown in Figure 4.4:

Level 1: A circular ROI was drawn for liver left lobe (LL), spleen (SPL)

Level 2: A circular ROI was drawn for liver right lobe (RL), aorta (A), left kidney (LK)

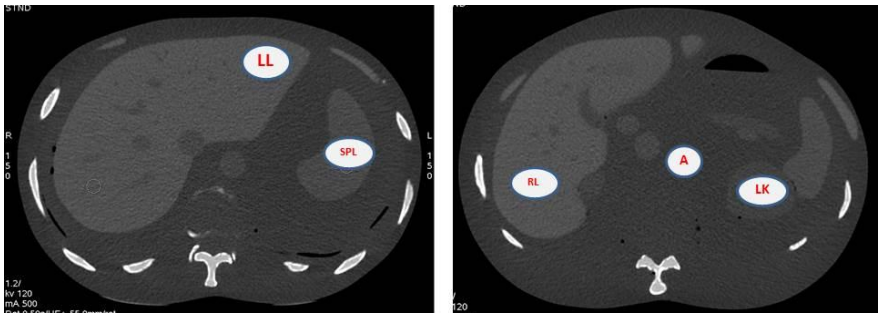

Level 1 **Level 2**

Figure 4.5 Two images at 2 levels were selected for noise measurements in 5 volume tissues as defined.

4.2.5 Noise Index (NI) is Image Quality Parameter which sets the image noise in the image. To determine the relationship between NI and radiation dose at a given reconstruction slice thickness, between 2 GE CT scanners, measured standard deviation or noise index (NI) from 5 selected 100 mm2 region of interest (ROI) of the 5 volume tissues as defined in 4.2.4 were recorded.

4.2.6 Estimation of Effective dose (E_{DLP})

The console-displayed DLP for all selected protocols were recorded for further estimation of effective doses. The dose–length product (DLP) is directly proportional to the patient's effective dose. Dividing the effective dose by the DLP yields a conversion factor, E/DLP ratio or *k coefficient* for specific type of examinations that can be used to convert DLP data at the completion of the CT scan into a corresponding estimate of effective dose[16]. The E/DLP ratio or *k coefficient* is expressed as $mSv\ mGy^{-1}\ cm^{-}$. Effective dose in CT (E_{DLP}) is given as:

$$E_{DLP} = DLP \times k$$

The values of *k* are dependent only on the region of the body being scanned (head, neck, thorax, abdomen, or pelvis). Normalized effective dose per dose-length product (DLP) "k" for standard size adults and pediatric patients of various ages over various body regions is shown in Table 4.1[17.] Using this method, *E* can be estimated from the DLP, which is reported on most CT systems.

Table 4.1 Published DLP to E "k" Conversion Coefficients[18]

Region of the Body	*k ($mSv\ mGy^{-1}\ cm^{-1}$)*				
	0 year old	*1 year old*	*5 year old*	*10 year old*	*Adult*
Head and neck	0.013	0.0085	0.0057	0.0042	0.0031
Head	0.011	0.0067	0.0040	0.0032	0.0021
Neck	0.017	0.012	0.011	0.0079	0.0059
Chest	0.039	0.026	0.018	0.013	0.014
Abdomen ≈& pelvis	0.049	0.030	0.020	0.015	0.015
Trunk	0.044	0.028	0.019	0.014	0.015

E_{DLP} is only valid for a reference-sized individual who weighs approximately 70 kg. When scanning patients whose size differs from assuming normal-sized adult patient, it will be important to use appropriate correction factors to obtain a more reliable patient effective dose. With recent development of methods to estimate patient organ dose in CT using size-specific dose estimates (SSDE) [19].

CHAPTER V
RESULTS AND DISCUSSION

5.1 Relationships between NI values and radiation dose

At a constant slice thickness, 1.25 mm for both 64-MDCT LightSpeed VCT and HDCT Discovery 750HD scanners, relationships between Noise Index (NI) values and radiation dose are shown in Table 5.1 and 5.2 Radiation measurements performed using 3 sizes of body phantom, standard, large and very large. NI values measured from 5 selected 100 mm^2 region of interest (ROI) of the 5 volume tissues, Right Liver lobe (RL), Left Liver lobe (LL), Left kidney (LK), Spleen (SPL), and Aorta (A). The CT dose index of volume ($CTDI_{vol}$) and dose-length product (DLP) were recorded, and the mean value was calculated. The dose-length product was converted to the effective dose.

Table 5.1 Relationship between NI values and radiation dose for averaged phantom at a constant reconstruction slice thickness, 1.25 mm for MDCT.

Scanner	HDCT Discovery 750HD											
Phantom size	Standard				Large				Very large			
Noise Index	0	10	15	20	0	10	15	20	0	10	15	20
Tissue ROI	Measured Noise Index											
RL	19.1	16.27	18.05	19.15	21.00	17.25	20.4	21.85	22.53	19.2	22.00	22.55
LL	14.4	15.65	18.05	18.7	16.1	17.5	18.75	19.5	19.55	22.25	20.4	20.9
LK	16.35	17.00	15.6	18.9	18.85	17.9	15.9	19.95	20.65	19.2	19.4	20.6
SPL	16.3	16.00	13.7	16.2	17.35	18.2	16.4	17.75	18.7	20.00	19.15	18.15
A	20.1	19.5	20.9	21.4	22.8	21.9	22.1	22.15	23.3	25.3	24.55	26.05
Dose (mSv)	6.86	6.87	6.60	4.57	6.87	6.86	6.82	5.36	6.87	6.87	6.87	6.44

Both scanners showed similar patterned of measured noise and estimated radiation dose. At reference noise index from 0 to 20, the measured noise values increased with increasing phantom sizes. When reference noise index was set at 20, the estimated effective dose was lowest for all sizes of phantom. Increasing noise index means higher noise in the image resulting in decreasing radiation dose. For very large sized phantom, as the reference NI was increased to 20, change in radiation dose radiation dose was less than those from standard and large sized phantom. Dose change from NI 15 to NI 20 for standard, large and very large sized phantom were 30.75, 21.40 and 6.26% for MDCT; 37.30, 33.13 and 24.27% for HDCT respectively (Table 5.1 and 5.2).

Table 5.2 Relationship between NI values and radiation dose for averaged phantom at a constant reconstruction slice thickness, 1.25 mm for HDCT.

Scanner	HDCT Discovery 750HD											
Phantom size	Standard				Large				Very large			
Noise Index	0	10	15	20	0	10	15	20	0	10	15	20
Tissue ROI	Measured Noise Index											
RL	19.00	17.7	16.05	21.4	21.1	19.4	20.15	22.55	22.27	22.2	22.7	22,75
LL	15.2	14.85	16.5	19.15	19.25	19.3	18.6	22.2	23.35	22.5	22.1	24.5
LK	16.00	17.6	16.8	18.5	18.75	18.00	17.5	21.1	21.00	20.2	18.7	22.4
SPL	16.6	17.35	17.2	23.25	18.1	21.25	18.65	25.5	21.00	22.14	24.25	26.65
A	20.95	21.85	19.6	27.1	24.95	23.8	22.85	27.55	27.1	24.95	23.95	31.9
Dose (mSv)	6.88	6.87	5.87	3.68	6.81	6.87	6.61	4.42	6.88	6.88	6.88	5.21

Tissue ROIs: RL, LL, A, SPL and LK showed lowest measured noise index at reference noise index 15 for all sized of phantom.

For very large sized phantom, measured NI was high for all reference NI values from 0 to 20. These 2 tables show that scan parameters should be tailored fit to better match patient size in an effort to reduce dose. In this study, NI of 15 may considered the optimum NI for upper abdomen scan in all sizes of phantom.

A comparison of estimated effective dose in tissue ROIs between MDCT and HDCT as a function of NI was shown in Table 5.3, 5.4 and 5.5 for standard, large and very large sized phantom respectively. As in Table 5.1 and 5.2, for all sizes of phantom, the lowest estimated effective dose was observed at NI 20.

Table 5.3 Relationships between noise index and radiation dose for standard sized phantom, a comparison between MDCT and HDCT scanners.

Phantom Size	Standard							
Scanner	MDCT	HDCT	MDCT	HDCT	MDCT	HDCT	MDCT	HDCT
Set noise index	0	0	10	10	15	15	20	20
RL	19.1	19.0	16.27	17.7	18.05	16.05	19.15	21.4
LL	14.4	15.2	15.65	14.85	18.05	16.5	18.7	19.15
LK	16.35	16.0	17.0	17.6	15.6	16.8	18.9	18.5
SPL	16.3	16.6	16.0	17.35	13.7	17.2	16.2	23.25
A	20.1	20.95	19.5	21.85	20.9	19.6	21.4	27.1
Dose(mSv)	6.86	6.88	6.87	6.87	6.6	5.87	4.57	3.68

Table 5.4 Relationships between noise index and radiation dose for large sized phantom, a comparison between MDCT and HDCT scanners.

Phantom Size	Large							
Scanner	MDCT	HDCT	MDCT	HDCT	MDCT	HDCT	MDCT	HDCT
Set noise index	0	0	10	10	15	15	20	20
RL	21	21.1	17.25	19.4	20.4	20.15	21.85	22.55
LL	16.1	19.25	17.5	19.3	18.75	18.6	19.5	22.2
LK	18.85	18.75	17.9	18	15.9	17.5	19.95	21.1
SPL	17.35	18.1	18.2	21.25	16.4	18.65	17.75	25.5
A	22.8	24.95	21.9	23.8	22.1	22.85	22.15	27.55
Dose(mSv)	6.87	6.81	6.86	6.87	6.82	6.61	5.36	4.42

Table 5.5 Relationships between noise index and radiation dose for very large sized phantom, a comparison between MDCT and HDCT scanners.

Phantom Size	Overlarge							
Scanner	MDCT	HDCT	MDCT	HDCT	MDCT	HDCT	MDCT	HDCT
Set noise index	0	0	10	10	15	15	20	20
RL	22.53	22.27	19.2	22.2	22	22.7	22.55	22.75
LL	19.55	23.35	22.25	22.5	20.4	22.1	20.9	24.5
LK	20.65	21	19.2	20.2	19.4	18.7	20.6	22.4
SPL	18.7	21	20	22.14	19.15	24.25	18.15	26.65
A	23.3	27.1	25.3	24.95	24.55	23.95	26.05	31.9
Dose(mSv)	6.87	6.88	6.87	6.88	6.87	6.88	6.44	5.21

5.2 Relationships between NI values and phantom sizes as a function of slice thickness

Figure 5.1 to 5.2.40 showed relationships between NI values and phantom sizes at slice thicknesses, 1.25 mm and 7 mm. Radiation measurements were performed on 64-MDCT LightSpeed VCT and HDCT Discovery 750HD scanners using 3 sizes of body phantom. Added bolus material to the abdomen of an anthropomorphic phantom simulates patients of three sizes: standard, large, and very large size. Measured NI obtained from 5 selected 100 mm^2 region of interest (ROI) of the 5 volume tissues, Right Liver lobe (RL), Left Liver lobe (LL), Left kidney (LK), Spleen (SPL), and Aorta (A) from MCDT and HDCT were compared.

Both MDCT and HDCT scanners showed similar patterns of measured noise index (NI). Measured NI was found to increase progressively as size of phantom increase but decrease with the increase of slice thickness. A slice thickness of 7 mm gave lower measured NI values than 1.25 mm. As NI is an image quality parameter which sets the image noise in the image. Measured NI will vary based on the slice thickness selected due to the fact that difference in image noise relative to slice thickness. Increasing Noise Index means higher noise in the image which resulting in decreasing radiation dose.

RIGHT LOPE LIVER Slice thickness 1.25 mm

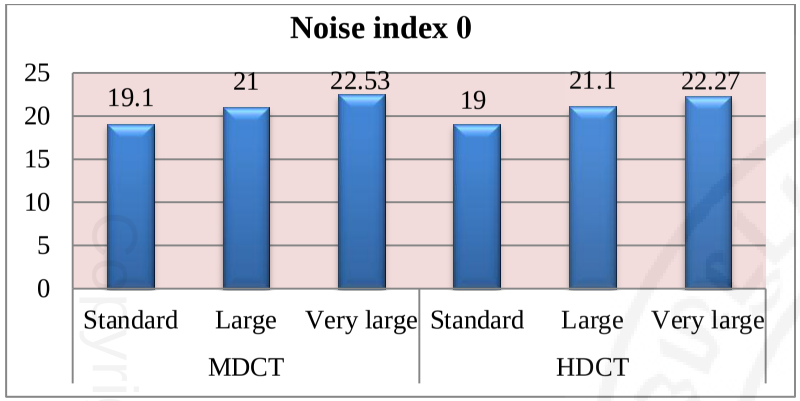

Figure 5.1 NI 0, Right liver lobe, 1.25 mm

RIGHT LOPE LIVER Slice thickness 7 mm

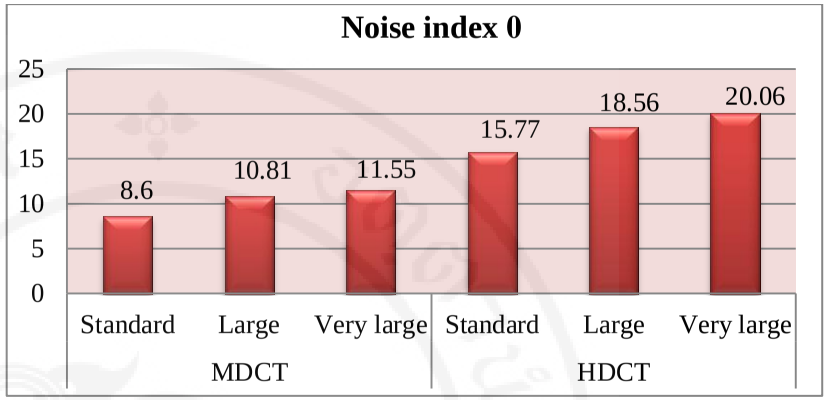

Figure 5.2 NI 0, Right liver lobe, 7 mm

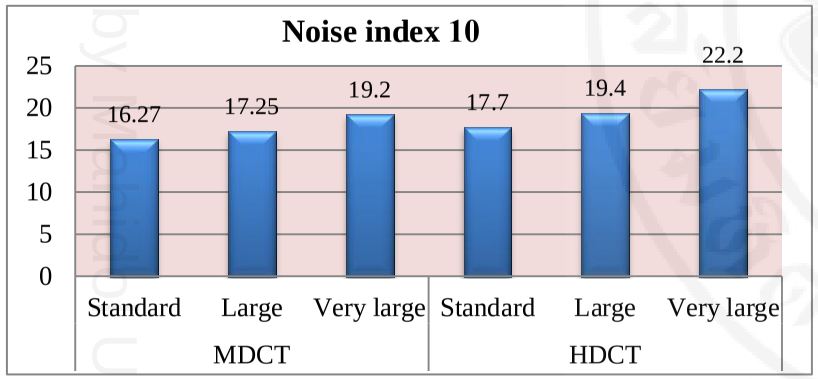

Figure 5.3 NI 10, Right liver lobe, 1.25 mm

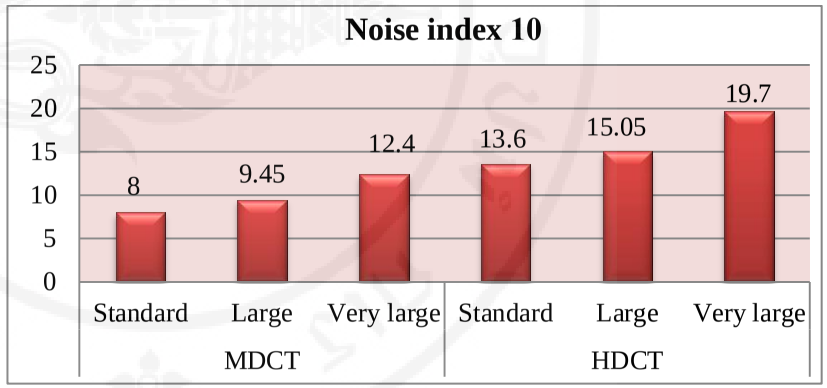

Figure 5.4 NI 0, Right liver lobe, 7 mm

RIGHT LOPE LIVER Slice thickness 1.25 mm

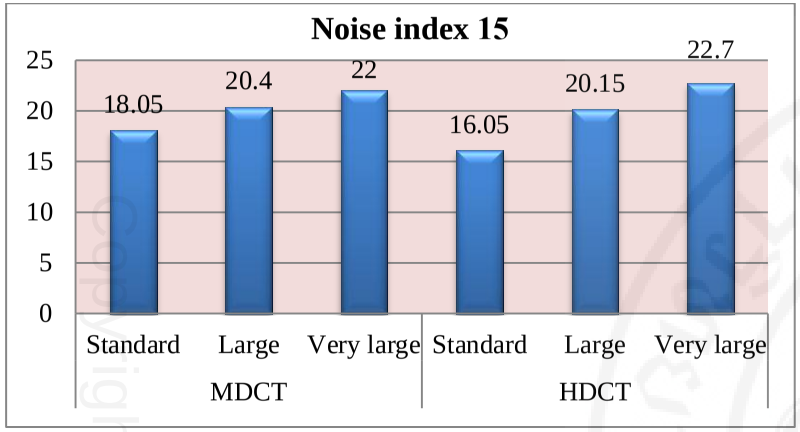

Figure 5.5 NI 15, Right liver lobe, 1.25 mm

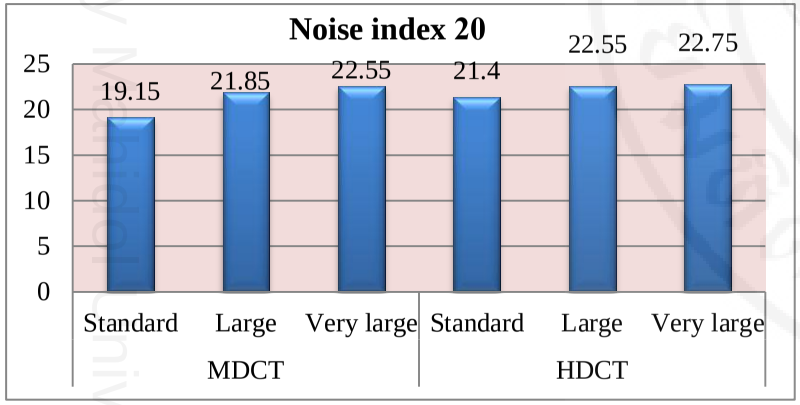

Figure 5.7 NI 20, Right liver lobe, 1.25 mm

RIGHT LOPE LIVER Slice thickness 7 mm

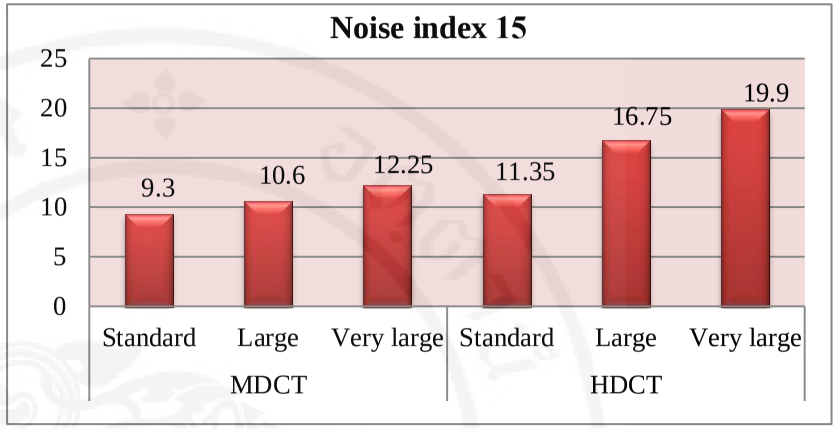

Figure 5.6 NI 14, Right liver lobe, 7 mm

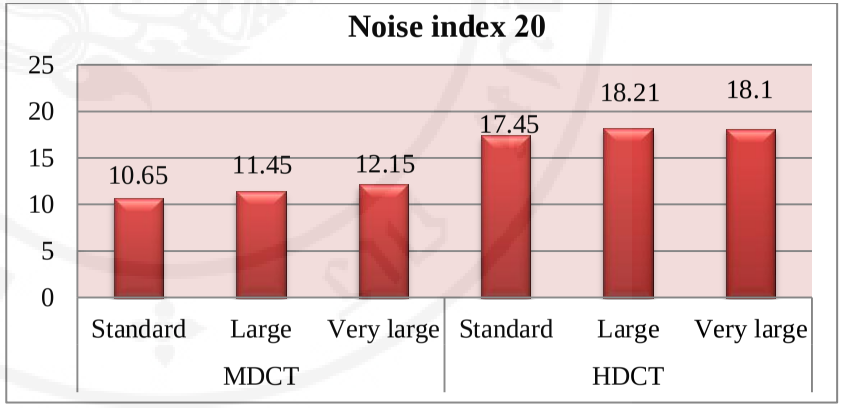

Figure 5.8 NI 20, Right liver lobe, 7 mm

LEFT LOPE LIVER Slice thickness 1.25 mm

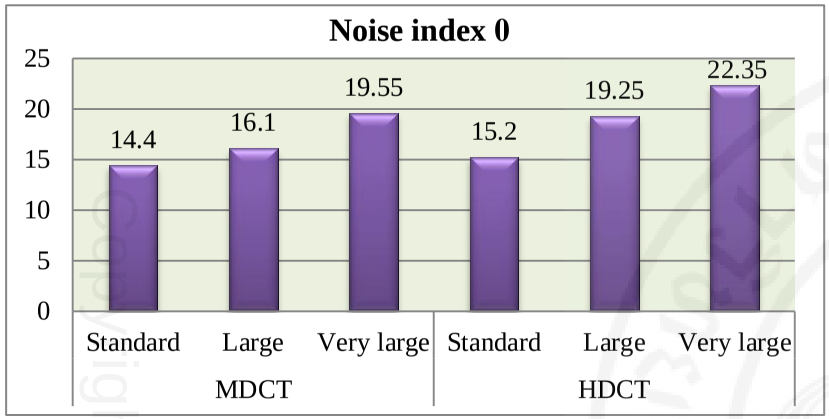

Figure 5.9 NI 0, Left liver lobe, 1.25 mm

LEFT LOPE LIVER Slice thickness 7 mm

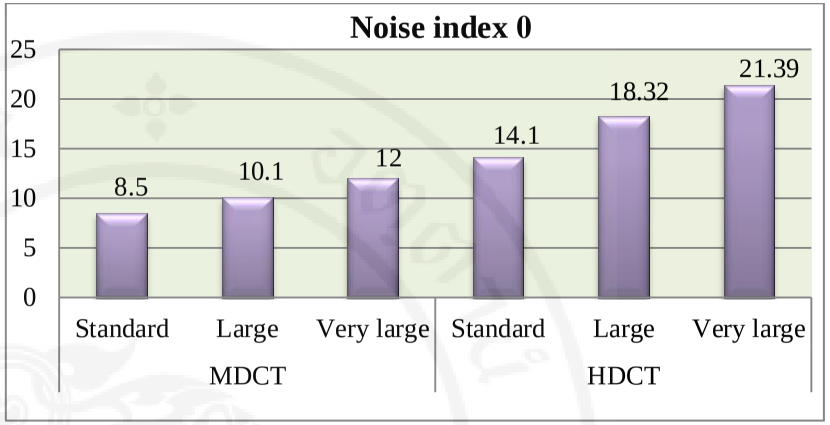

Figure 5.10 NI 0, Left liver lobe, 7 mm

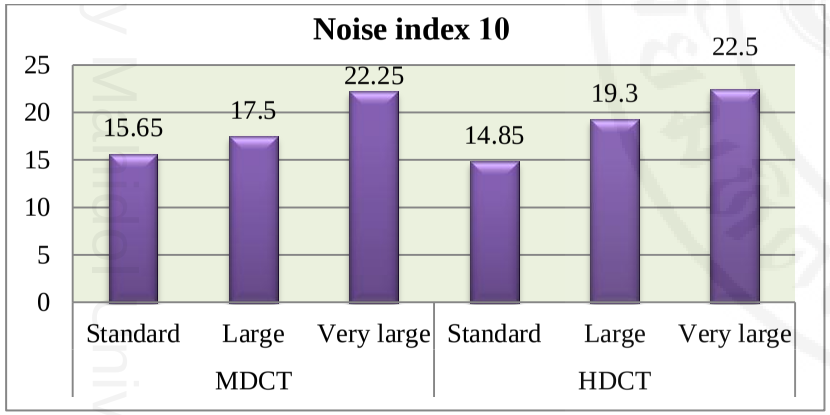

Figure 5.11 NI 10, Left liver lobe, 1.25 mm

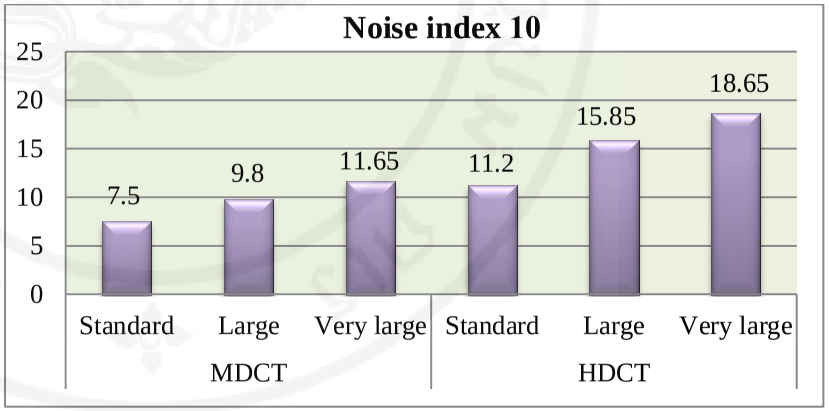

Figure 5.12 NI 10, Left liver lobe, 7 mm

LEFT LOPE LIVER Slice thickness 1.25 mm

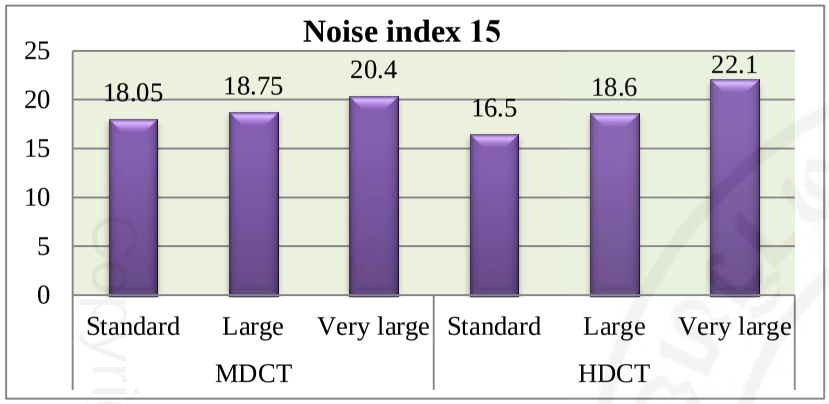

Figure 5.13 NI 15, Left liver lobe, 1.25 mm

LEFT LOPE LIVER Slice thickness 7 mm

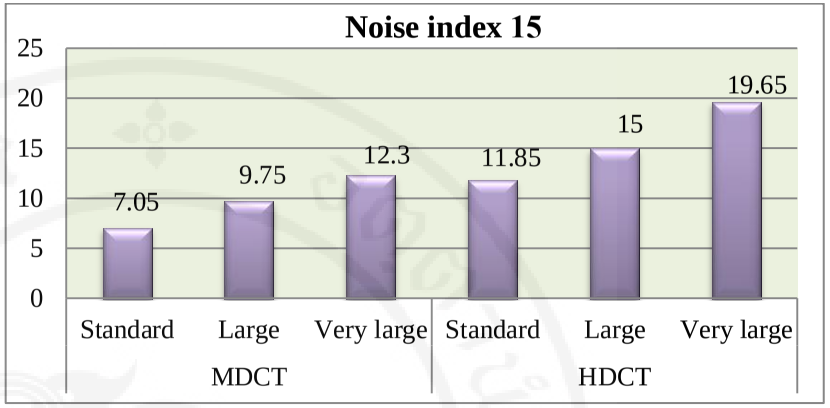

Figure 5.14 NI 15, Left liver lobe, 7 mm

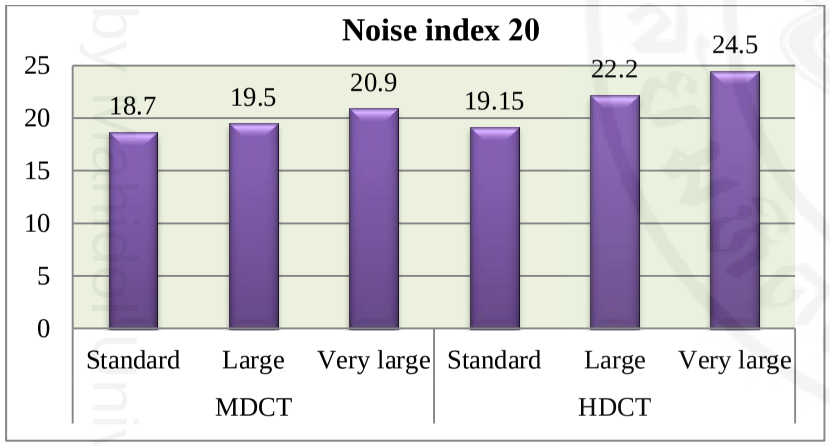

Figure 5.15 NI 20, Left liver lobe, 1.25 mm

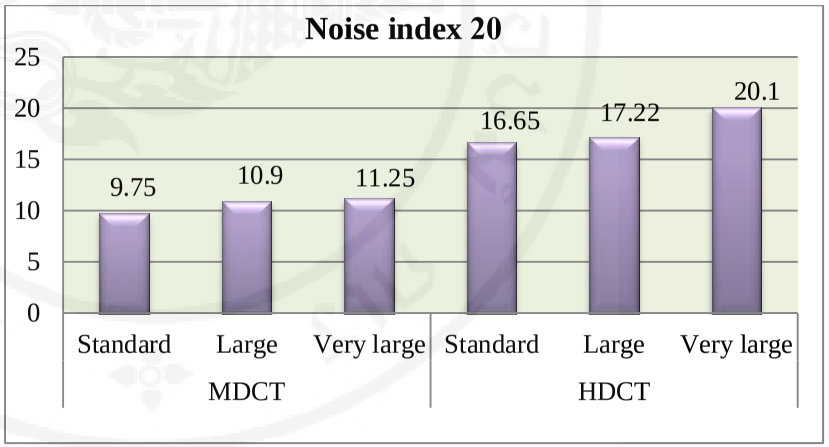

Figure 5.16 NI 20, Left liver lobe, 7 mm

SPLEEN Slice thickness 1.25 mm

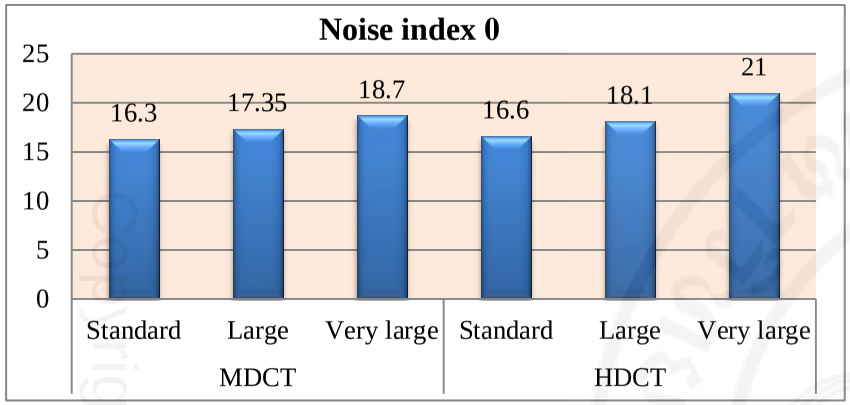

Figure 5.17 NI 0, Spleen, 1.25 mm

SPLEEN Slice thickness 7 mm

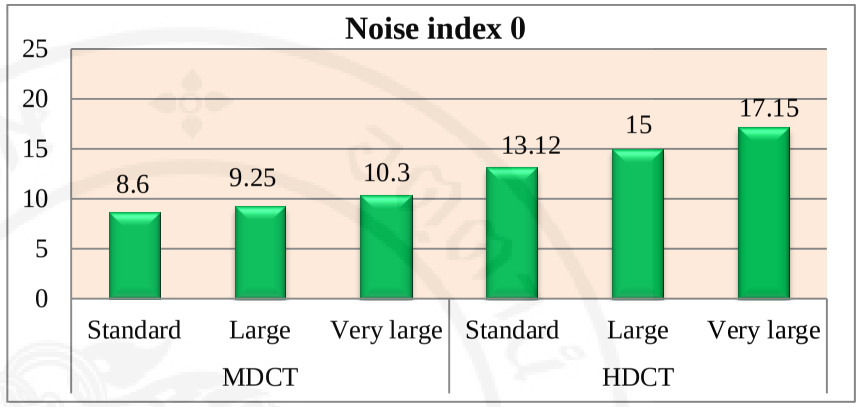

Figure 5.18 NI 0, Spleen, 7 mm

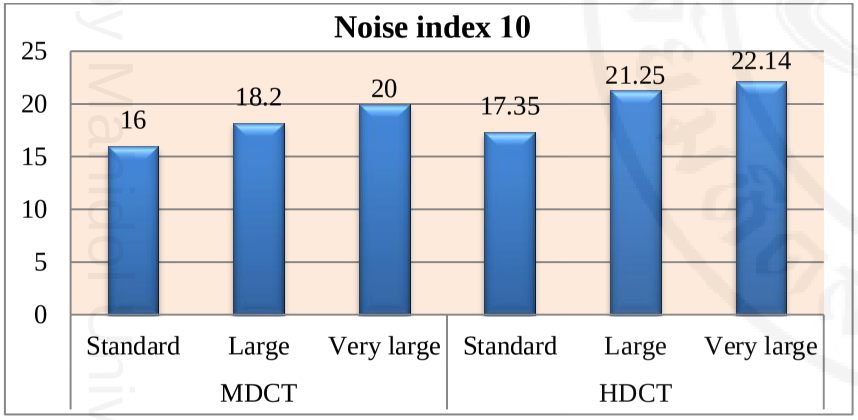

Figure 5.19 NI 10, Spleen, 1.25 mm

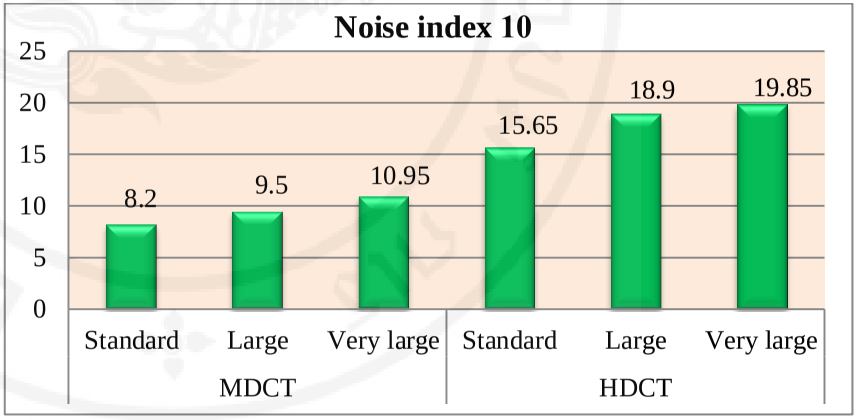

Figure 5.20 NI 10, Spleen, 1.25 mm

SPLEEN Slice thickness 1.25 mm

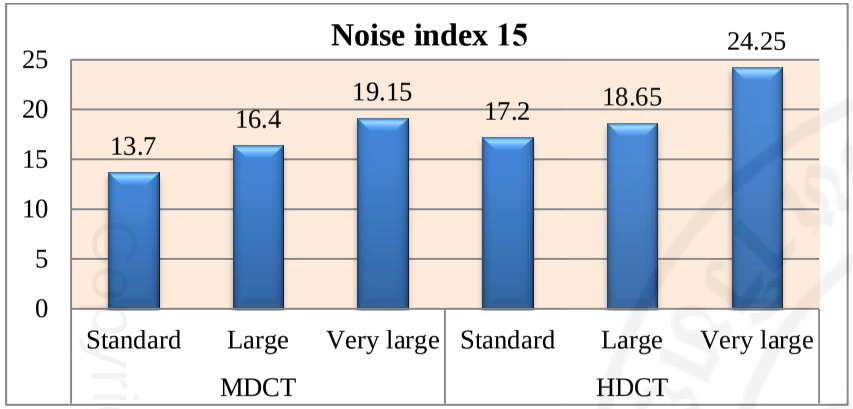

Figure 5.21 NI 15, Spleen, 1.25 mm

SPLEEN Slice thickness 7 mm

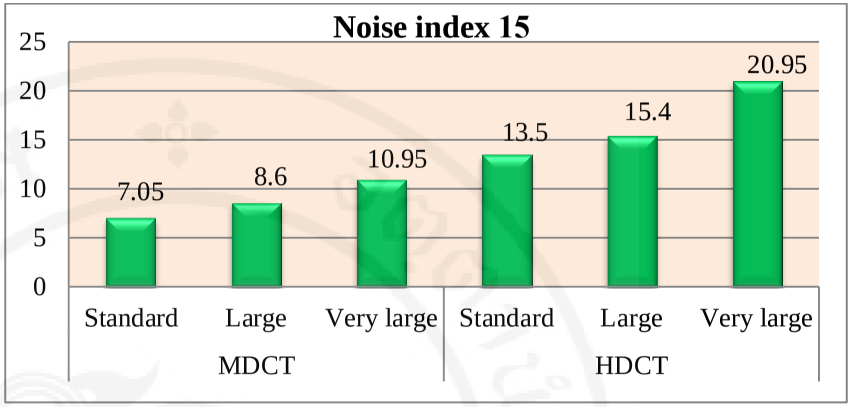

Figure 5.22 NI 15, Spleen, 7 mm

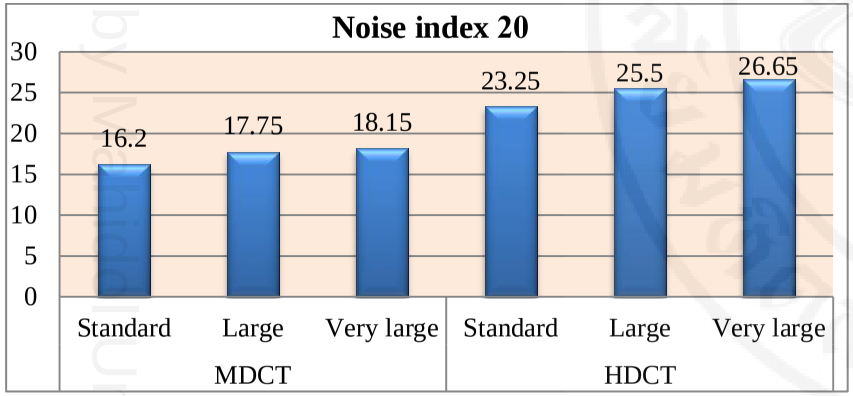

Figure 5.23 NI 20, Spleen, 1.25 mm

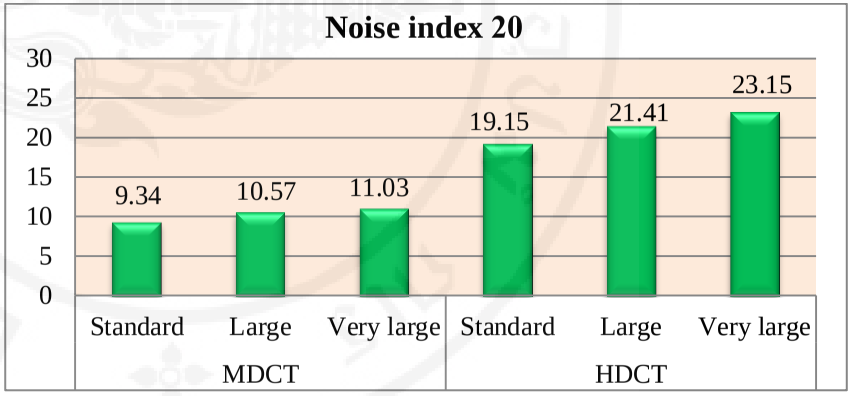

Figure 5.24 NI 20, Spleen, 7 mm

AORTA Slice thickness 1.25 mm

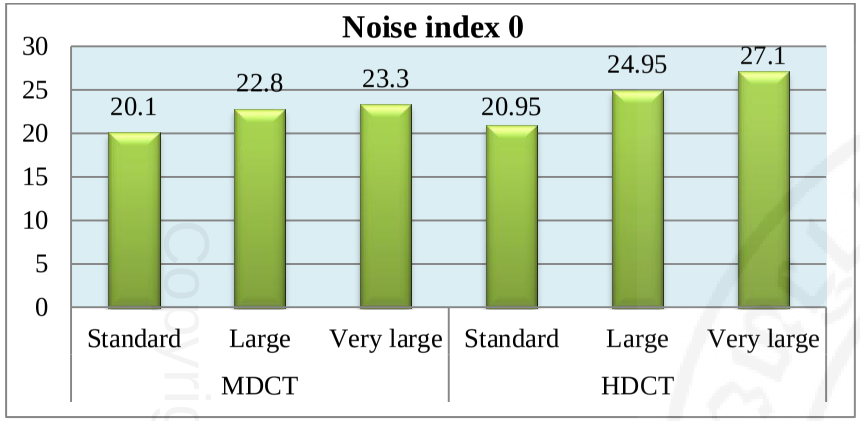

Figure 5.25 NI 0, Aorta, 1.25 mm

AORTA Slice thickness 7 mm

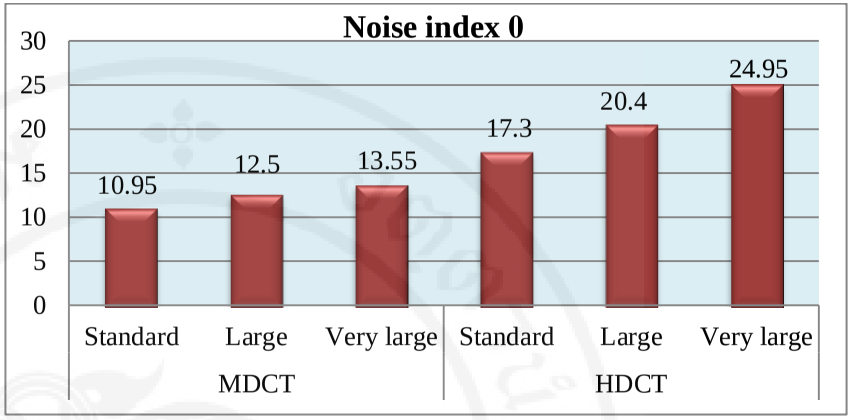

Figure 5.26 NI 0, Aorta, 7 mm

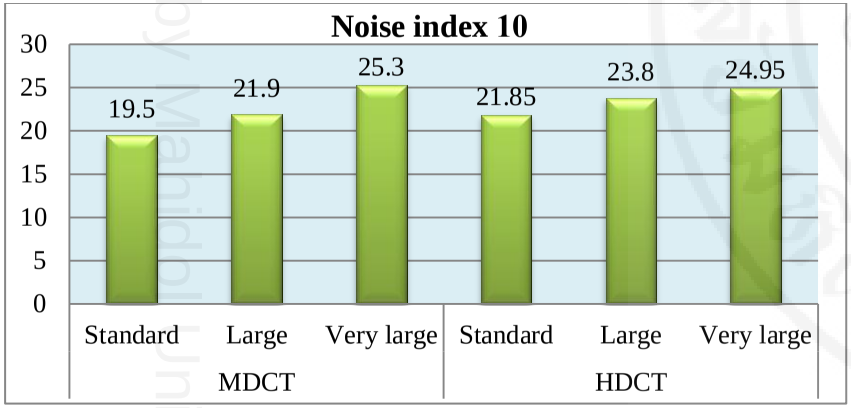

Figure 5.27 NI 10, Aorta, 1.25 mm

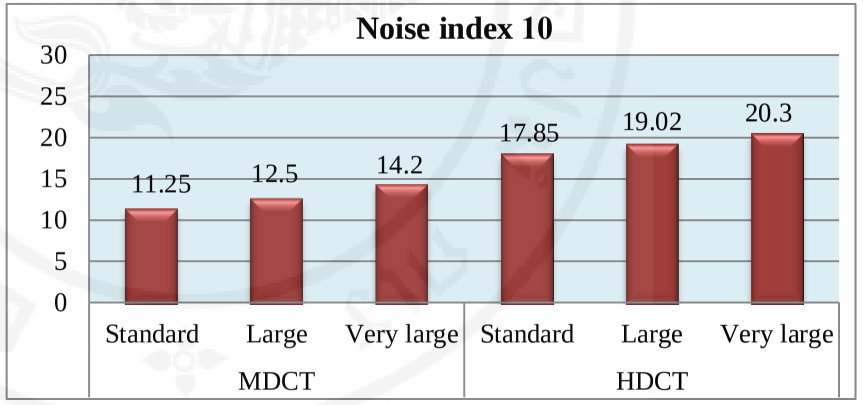

Figure 5.28 NI 10, Aorta, 7 mm

AORTA Slice thickness 1.25 mm

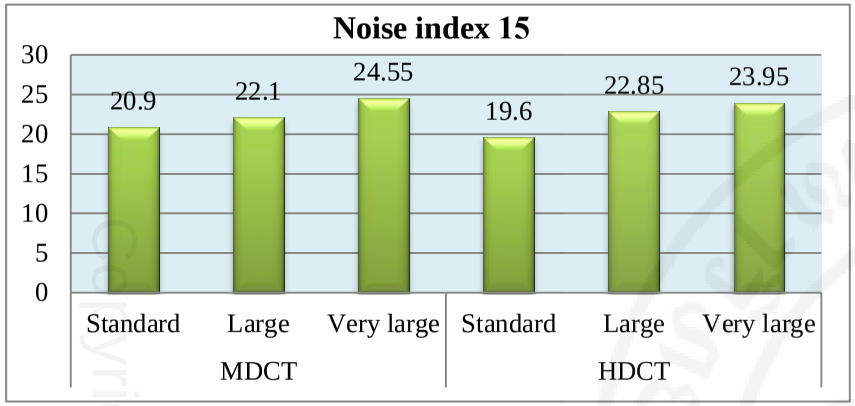

Figure 5.29 NI 15, Aorta, 1.25 mm

AORTA Slice thickness 7 mm

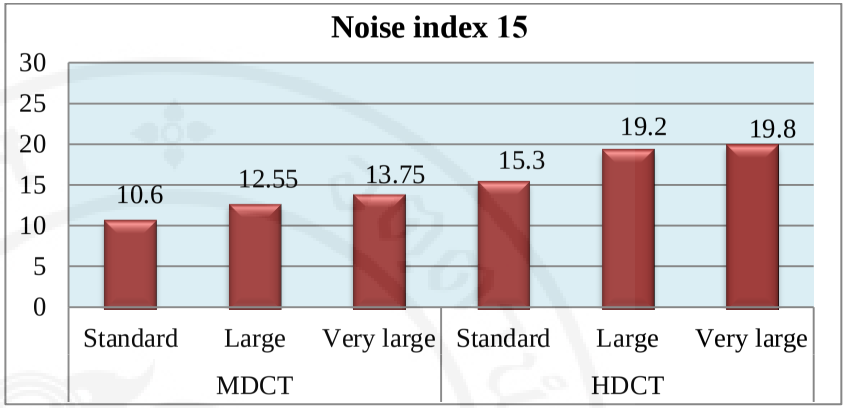

Figure 5.30 NI 15, Aorta, 7 mm

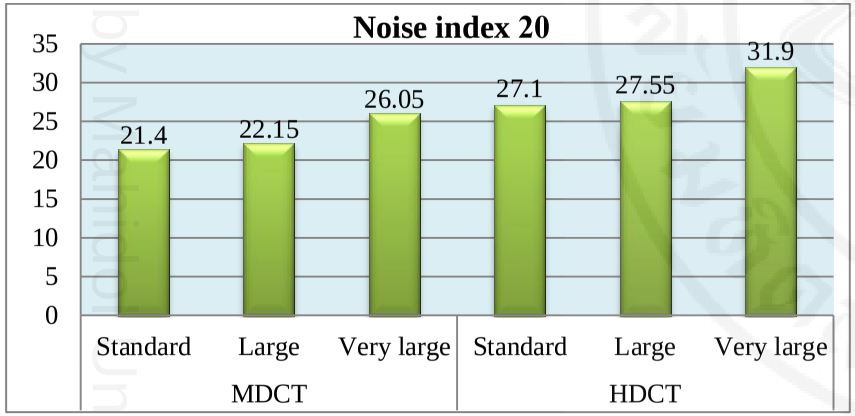

Figure 5.31 NI 20, Aorta, 1.25 mm

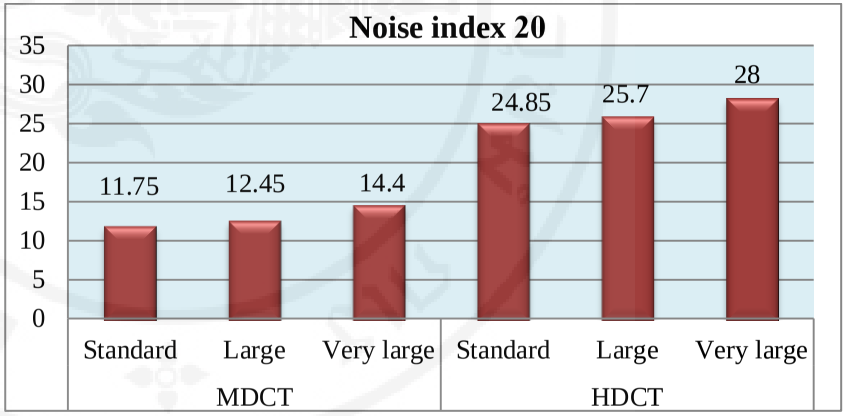

Figure 5.32 NI 20, Aorta, 7 mm

LEFT KIDNEY Slice thickness 1.25 mm

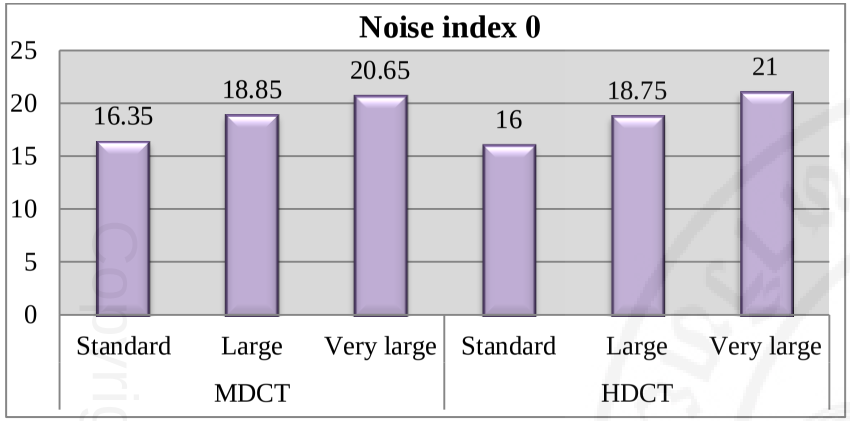

Figure 5.33 NI 0, Left kidney, 1.25 mm

LEFT KIDNEY Slice thickness 1.25 mm

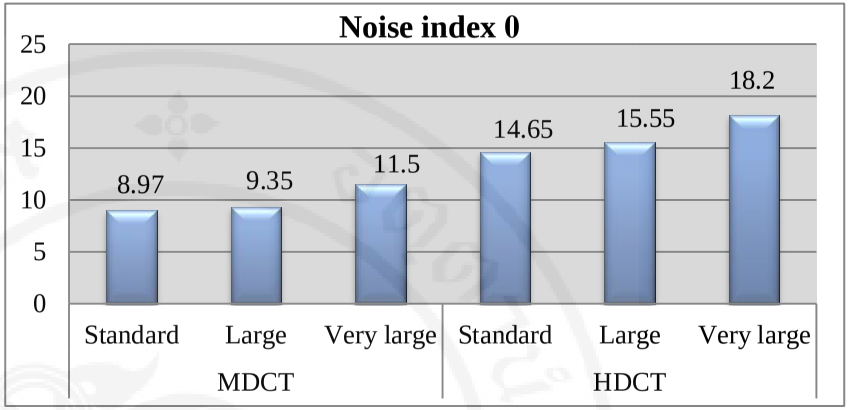

Figure 5.34 NI 0, Left kidney, 7 mm

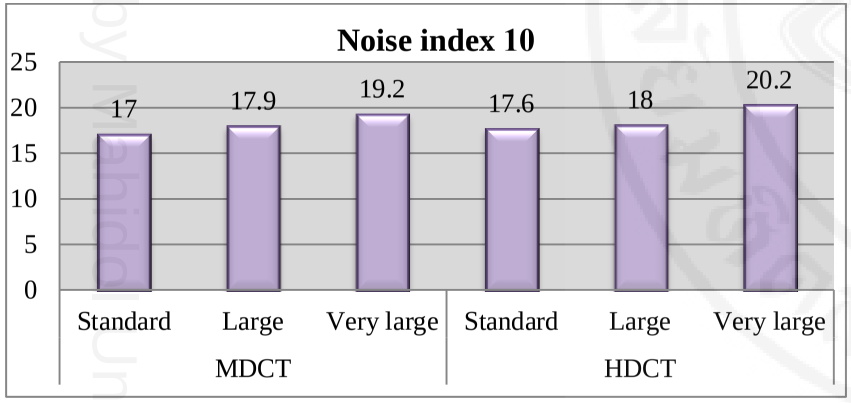

Figure 5.35 NI 10, Left kidney, 1.25 mm

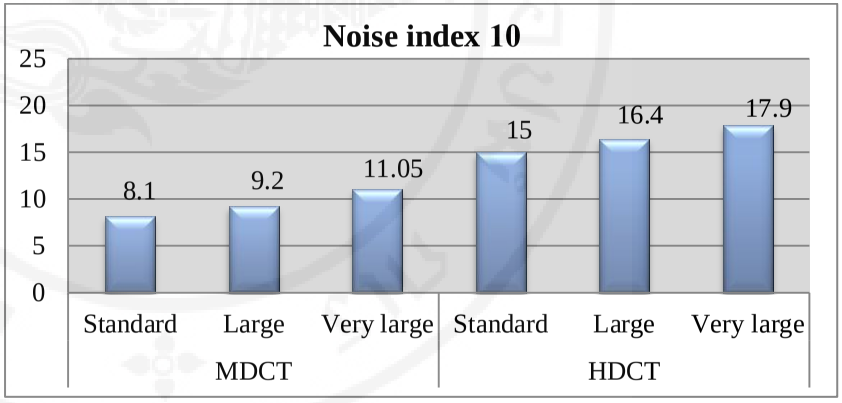

Figure 5.36 NI 10, Left kidney, 7 mm

LEFT KIDNEY Slice thickness 1.25 mm

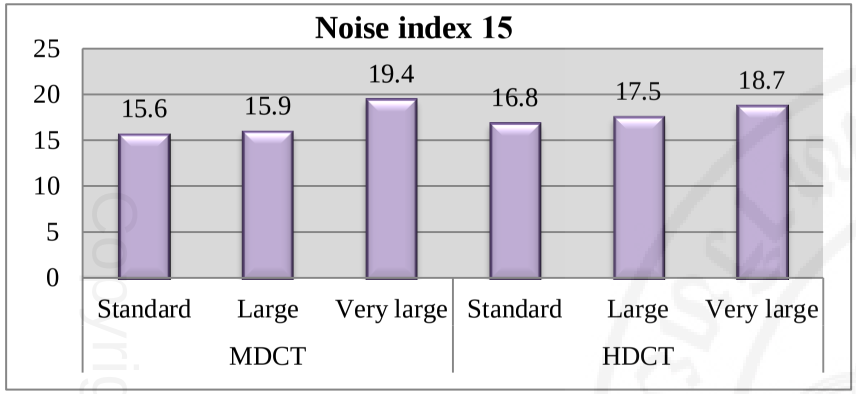

Figure 5.37 NI 15, Left kidney, 1.25 mm

LEFT KIDNEY Slice thickness 1.25 mm

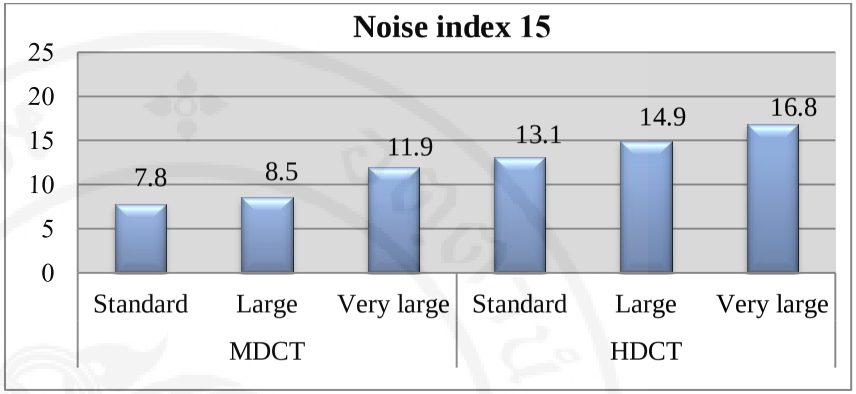

Figure 5.38 NI 15, Left kidney, 7 mm

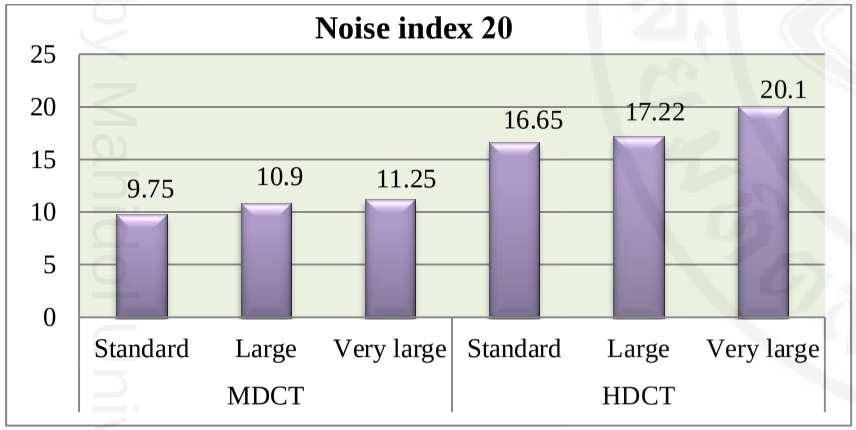

Figure 5.39 NI 20, Left kidney, 1.25 mm

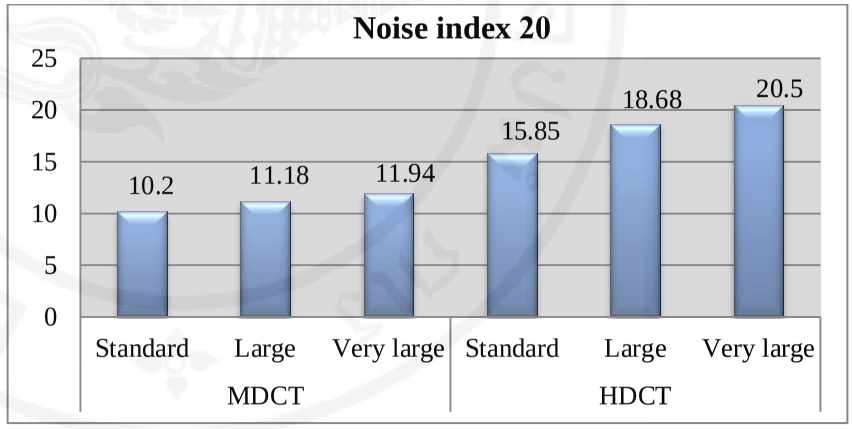

Figure 5.40 NI 20, Left kidney, 7 mm

5.3 Noise Index as a function of application for improving image quality

Scanner 1 MDCT: Filtered back projection (FBP)

Scanner 2 HDCT: GE*'s model based iterative reconstruction (MBIR) technology or Veo*, and Adaptive Statistical Iterative Reconstruction (ASIR).

Table 5.6, 5.7, 5.8, 5.5.4 and 5.5.5 demonstrated relationships between NI and phantom sizes at a constant slice thickness, 1.25 mm for 5 selected tissue ROIs: Right Liver lobe (RL), Left Liver lobe (LL), Left kidney (LK), Spleen (SPL), and Aorta (A), as a function of image reconstruction applications for improving image quality; original NI (FBP), 30% ASIR, 40%ASIR, 50%ASIR and MBIR. These relationships were also graphically shown in Figure 5.6 to 5.10

Table 5.6 Relationships between noise index for 3 phantom sizes at a constant slice thickness, 1.25 mm for tissue ROI: Right Lobe Liver (RL) as a function of application for improving image quality.

Size of phantom	Noise index	RL				
		Thickness 1.25 mm				
		Original NI FBP	ASIR30	ASIR40	ASIR50	MBIR
Standard	0	15.6	15.11	13.75	12.45	8.85
	10	15.65	15.45	15.3	13.8	9.8
	15	16.7	16.5	16.2	14.44	10.12
	20	19.2	18.85	17.35	16.55	11.05
Large	0	17.85	16.8	15.35	15.05	9.95
	10	19.05	18.06	16.5	15.4	10
	15	19.9	18.7	17.15	15.6	11.1
	20	21.4	18.95	17.9	15.95	12.4
Very large	0	20.65	19.55	16.9	16.55	9.71
	10	21	19.57	18	17.01	12.15
	15	22.3	20.4	18.35	17.3	14.4
	20	23.8	22	21	18.3	15.45

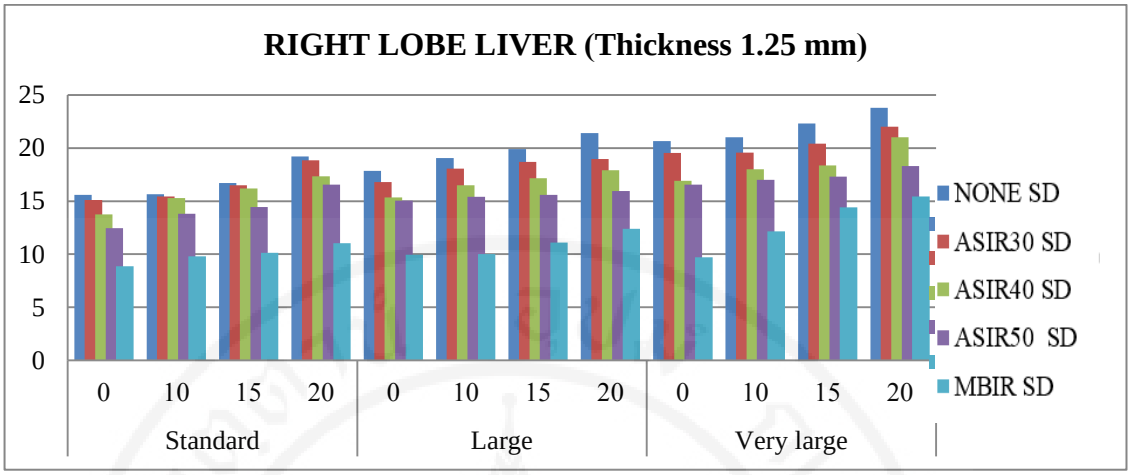

Figure 5.41 Noise index from 3 phantom sizes at a constant slice thickness, 1.25 mm for tissue ROI: Right Lobe Liver (RL) as a function of application for improving image quality.

Table 5.7 Relationships between noise index for 3 phantom sizes at a constant slice thickness, 1.25 mm for tissue ROI: Left Lobe Liver (LL) as a function of application for improving image quality.

Size of phantom	Noise index	LL				
		Thickness 1.25 mm				
		Original NI FBP	ASIR30	ASIR40	ASIR50	MBIR
Standard	0	16.55	14.85	12.5	12.05	9.9
	10	17.05	16.15	14.75	13.8	10.09
	15	17.5	16.65	15.5	15.1	11.05
	20	18.2	18	16.65	16.4	11.7
Large	0	18.65	16.25	14.8	14.5	11.9
	10	18.85	17.75	15.46	15.01	12.67
	15	19.45	19	15.7	15.5	14.5
	20	22.35	20.1	17.5	17.25	15.65
Very large	0	20.95	20.7	19.75	17.95	12.1
	10	22.2	21.32	19.89	18.38	13.15
	15	23.4	22.05	20.3	19.24	13.45
	20	25.05	23.27	22.2	20.25	15.7

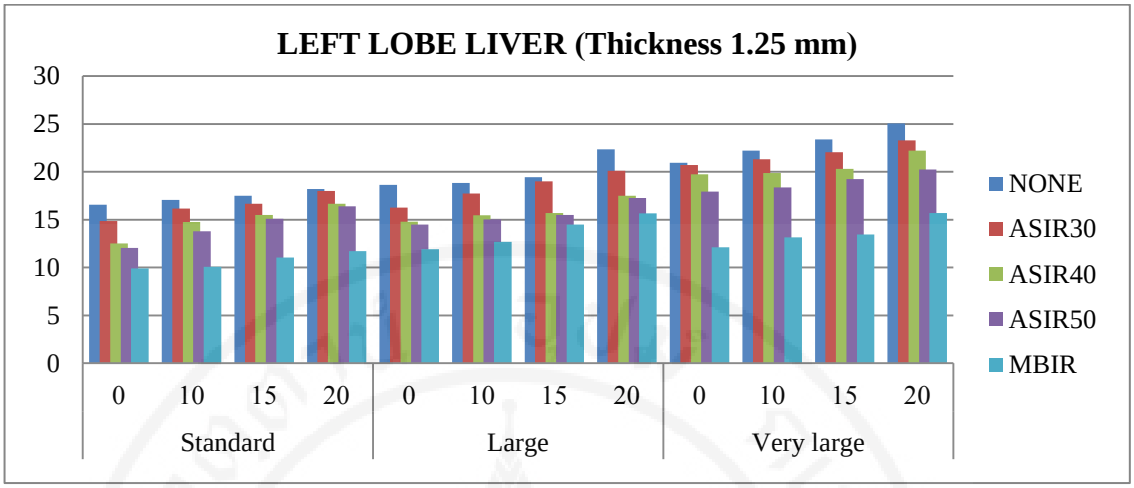

Figure 5.42 Noise index from 3 phantom sizes at a constant slice thickness, 1.25 mm for tissue ROI: Left Lobe Liver (LL) as a function of application for improving image quality.

Table 5.8 Relationships between noise index and phantom sizes at a constant slice thickness, 1.25 mm for tissue ROI: Aorta (A) as a function of application for improving image quality.

Size of phantom	Noise index	A				
		Thickness 1.25 mm				
		Original NI FBP	ASIR30	ASIR40	ASIR50	MBIR
Standard	0	17.93	17.4	16.8	15.35	10.63
	10	18.4	18.08	16.93	15.99	11.2
	15	20	19.35	17.65	16.45	12.7
	20	21.15	20.09	18.05	17.67	12.95
Large	0	19.5	17.3	16.45	15.35	13.65
	10	20.8	18.95	17.5	16.2	15.5
	15	21.3	20	19.7	17.9	16.17
	20	22.4	21.25	20.38	18.05	17
Very large	0	22.9	22.4	20.6	17.8	14.65
	10	23.5	23	21.15	18.4	15.25
	15	25.5	23.2	21.41	19.95	17.15
	20	26.3	25.27	21.45	20.7	18.2

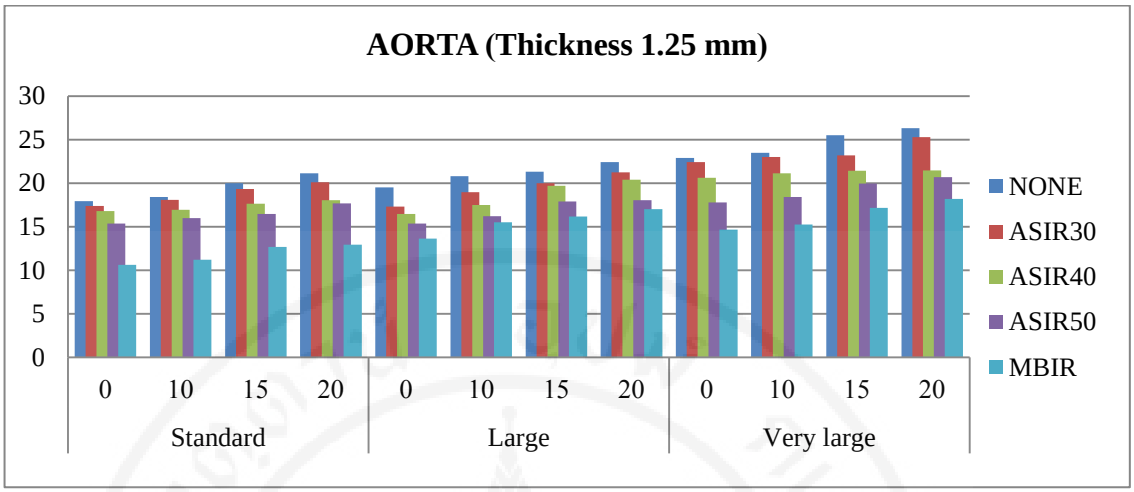

Figure 5.43 Noise index from 3 phantom sizes at a constant slice thickness, 1.25 mm for tissue ROI: Aorta (A) as a function of application for improving image quality.

Table 5.9 Relationships between noise index and phantom sizes at a constant slice thickness, 1.25 mm for tissue ROI: Spleen (SPL) as a function of application for improving image quality.

Size of phantom	Noise index	SPL				
		Thickness 1.25 mm				
		Original NI FBP	ASIR30	ASIR40	ASIR50	MBIR
Standard	0	17	13.79	12.8	11.57	9.02
	10	17.1	14.15	13	12.2	9.05
	15	17.15	15.1	13.45	12.45	9.15
	20	20	17.45	16.7	15.35	9.8
Large	0	17.2	15.5	14.9	14.4	9.25
	10	18.05	16.38	15.57	15.27	11.2
	15	21.29	19.95	19.6	18.1	11.4
	20	22.4	20.95	19.91	19.1	13.87
Very large	0	17.3	16.6	15.2	14.2	9.55
	10	18.95	17.3	16.2	15.8	12.1
	15	20.02	18.1	17.6	16.4	12.65
	20	21.55	19.3	18.7	15.8	13.2

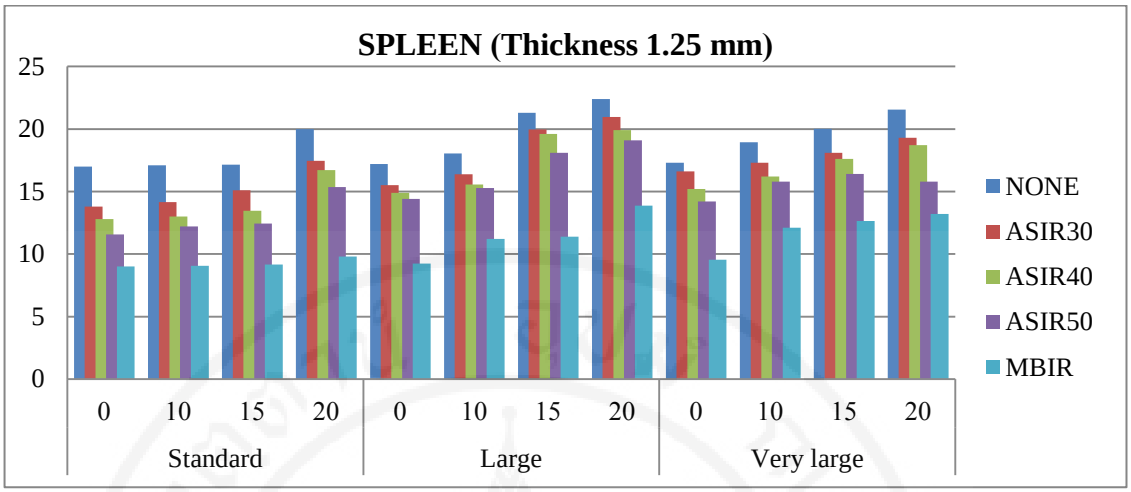

Figure 5.43 Noise index from 3 phantom sizes at a constant slice thickness, 1.25 mm for tissue ROI: Spleen (SPL) as a function of application for improving image quality.

Table 5.10 Relationships between noise index and phantom sizes at a constant slice thickness, 1.25 mm for tissue ROI: Left kidney (LK) as a function of application for improving image quality.

Size of phantom	Noise index	LK				
		Thickness 1.25 mm				
		Original NI FBP	ASIR30	ASIR40	ASIR50	MBIR
Standard	0	14.85	14.1	11.97	10.96	7.75
	10	15.1	14.38	12.71	11.25	8.2
	15	17.5	14.8	13.85	11.55	8.57
	20	18.7	17.35	15.95	14.95	11
Large	0	16.16	13.9	13.54	12.25	8.27
	10	16.4	14.76	14.1	13.46	8.47
	15	16.6	15	14.7	14	9.2
	20	17	15.4	15	14.9	11.3
Very large	0	16.9	16.6	15.5	14	8.8
	10	18	17.7	16.25	15.5	9.15
	15	18.55	18	17.35	16.2	9.5
	20	21.05	20	18.1	17.4	10.4

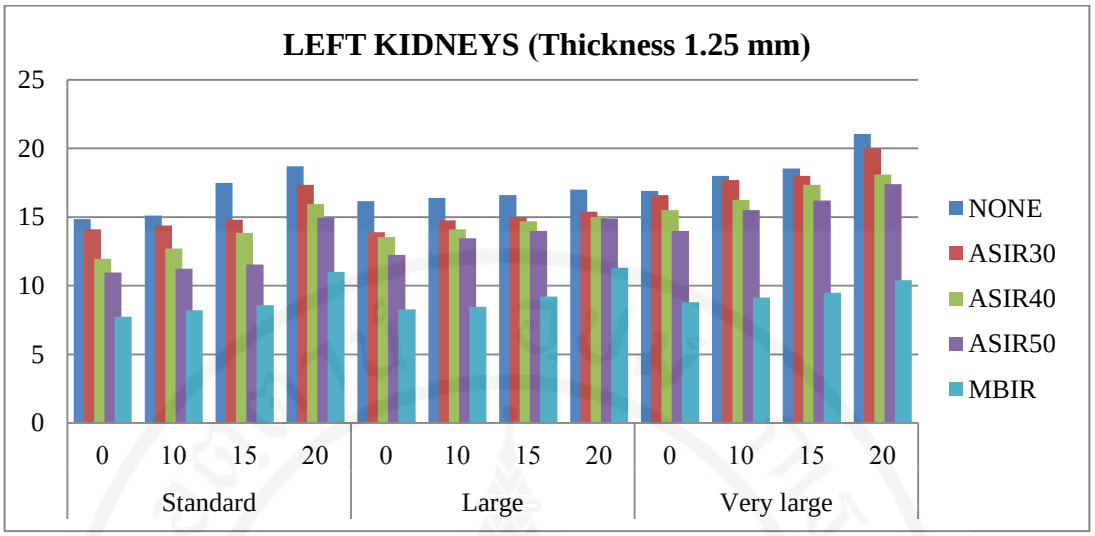

Figure 5.44 Noise index from 3 phantom sizes at a constant slice thickness, 1.25 mm for tissue ROI: Left kidney (LK) as a function of application for improving image quality.

Iterative reconstruction techniques have demonstrated the potential for improving image quality and reducing radiation dose in CT relative to the currently used filtered back projection techniques. In this phantom study, ASIR and MBIR provide diagnostic abdominal CT images with reduced image noise compared with FBP. The measured noise index for FBP, 30%ASIR, 40%ASIR, 50%ASIR and MBIR averaged from 5 selected tissues ROIs was shown in Table 5.11. They were 17.5±1.1, 16.4±1.5, 15.0±1.5, 14.0± 1.6, and 10.1±1.2 for standard-sized phantom which represented 6.75%, 14.08%, 20.20% and 42.22% reduction respectively, compared with FBP (mean=17.5±1.1).

For large-sized phantom, reduction in noise was greater with 30%ASIR, 40%ASIR, 50%ASIR and MBIR than with FBP. They were 19.3±1.7, 17.7±1.7, 16.6±1.6, 15.7± 1.3 and 12.2±2.5 which represented 8.19%, 14.2%, 19.0% and 37.0% reduction respectively, compared with FBP (mean=19.3±1.7) (Table 5.11).

For very large-sized phantom, the percentage of noise reduction was 6.43%, 13.1%, 20.1% and 38.5% with 30%ASIR, 40%ASIR, 50%ASIR and MBIR respectively when compared with FBP.

Table 5.11 Relationships between noise index and phantom sizes at a constant slice thickness, 1.25 mm as a function of 5 reconstructive techniques for improving image quality. Measured noise index was averaged from 5 selected tissue ROIs.

Size of phantom		Average from all tissue ROIs				
		Thickness 1.25 mm				
		Original NI FBP	ASIR30	ASIR40	ASIR50	MBIR
Standard	Mean	17.57	16.38	15.09	14.01	10.13
	SD	1.12	1.47	1.49	1.61	1.19
	% Reduction	-	6.75	14.08	20.21	42.34
Large	Mean	19.33	17.75	16.58	15.66	12.17
	SD	1.66	1.74	1.59	1.29	2.46
	% Reduction	-	8.19	14.20	19.00	37.00
Very large	Mean	21.66	20.27	18.82	17.31	13.32
	SD	2.22	2.48	1.97	1.77	1.83
	% Reduction	-	6.43	13.11	20.07	38.51

The effect of phantom size on noise reduction for different reconstructed methods is shown in Table 5.12. The percentage reduction of noise was comparable as the phantom size changed from standard to large and very large size, a similar trend was observed when FBP and ASIR techniques were used, but greater in MBIR. Noise reduction from standard to large size phantom were 9.96%, 8.36%, 9.87% and 11.70% for FBP, 30%ASIR, 40%ASIR and 50%ASIR respectively; from standard to very large size phantom were 23.28%, 23.75%, 24.72% and 23.47% for FBP, 30%ASIR, 40%ASIR and 50%ASIR respectively. For MBIR technique, the effect of phantom size on noise reduction was more noticeable, they were 20.14% and 30.49% as the phantom size changed from standard to large and very large size.

Table 5.12 The percentage reduction of noise for each reconstruction technique as a function of phantom size.

Size of phantom	Average from all tissue ROIs				
	Thickness 1.25 mm				
	Original NI FBP	ASIR30	ASIR40	ASIR50	MBIR
Standard	17.57	16.38	15.09	14.01	10.13
Large	19.33	17.75	16.58	15.66	12.17
Very large	21.66	20.27	18.82	17.31	13.32
	Noise reduction (%)				
Standard – Large	9.96	8.36	9.87	11.70	20.14
Standard – Verylarge	23.28	23.75	24.72	23.47	30.49

5.4 Console-displayed CT dose index of volume ($CTDI_{vol}$) and dose-length product (DLP)

Console displayed CT dose index of volume ($CTDI_{vol}$) and dose-length product (DLP) for MDCT were shown in Figure 5.47 (A, B and C) and for HDCT in Figure 5.49 The mean value was calculated. The dose-length product was converted to the effective dose as shown in Table 5.13 and Figure 5.50

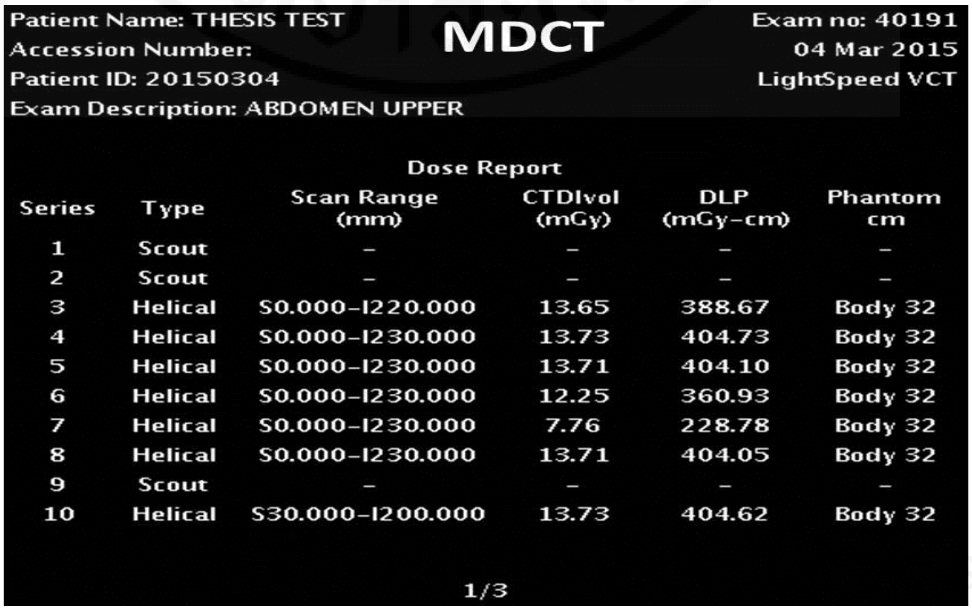
Patient Name: THESIS TEST
Accession Number:
Patient ID: 20150304
Exam Description: ABDOMEN UPPER

MDCT

Exam no: 40191
04 Mar 2015
LightSpeed VCT

Dose Report

Series	Type	Scan Range (mm)	CTDIvol (mGy)	DLP (mGy-cm)	Phantom cm
1	Scout	-	-	-	-
2	Scout	-	-	-	-
3	Helical	S0.000-I220.000	13.65	388.67	Body 32
4	Helical	S0.000-I230.000	13.73	404.73	Body 32
5	Helical	S0.000-I230.000	13.71	404.10	Body 32
6	Helical	S0.000-I230.000	12.25	360.93	Body 32
7	Helical	S0.000-I230.000	7.76	228.78	Body 32
8	Helical	S0.000-I230.000	13.71	404.05	Body 32
9	Scout	-	-	-	-
10	Helical	S30.000-I200.000	13.73	404.62	Body 32

1/3

Figure 5.46 (A) Console displayed CT dose index of volume (CTDIvol) and dose-length product (DLP) for MDCT

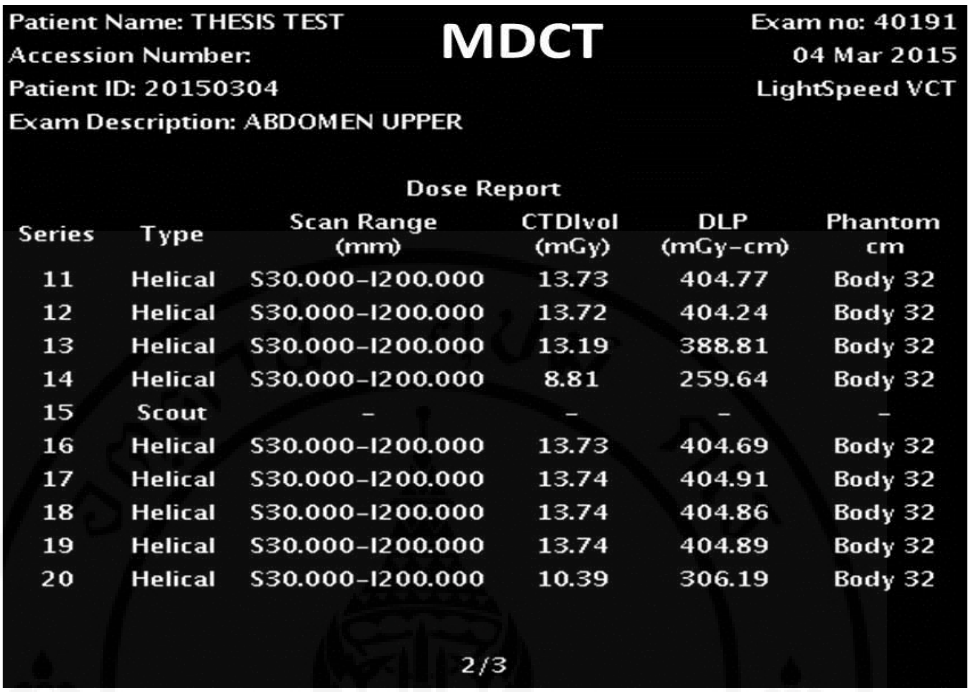

Patient Name: THESIS TEST
Accession Number:
Patient ID: 20150304
Exam Description: ABDOMEN UPPER

MDCT

Exam no: 40191
04 Mar 2015
LightSpeed VCT

Dose Report

Series	Type	Scan Range (mm)	CTDIvol (mGy)	DLP (mGy-cm)	Phantom cm
11	Helical	S30.000-I200.000	13.73	404.77	Body 32
12	Helical	S30.000-I200.000	13.72	404.24	Body 32
13	Helical	S30.000-I200.000	13.19	388.81	Body 32
14	Helical	S30.000-I200.000	8.81	259.64	Body 32
15	Scout	-	-	-	-
16	Helical	S30.000-I200.000	13.73	404.69	Body 32
17	Helical	S30.000-I200.000	13.74	404.91	Body 32
18	Helical	S30.000-I200.000	13.74	404.86	Body 32
19	Helical	S30.000-I200.000	13.74	404.89	Body 32
20	Helical	S30.000-I200.000	10.39	306.19	Body 32

2/3

Figure 5.47 (B) Console displayed CT dose index of volume ($CTDI_{vol}$) and dose-length product (DLP) for MDCT.

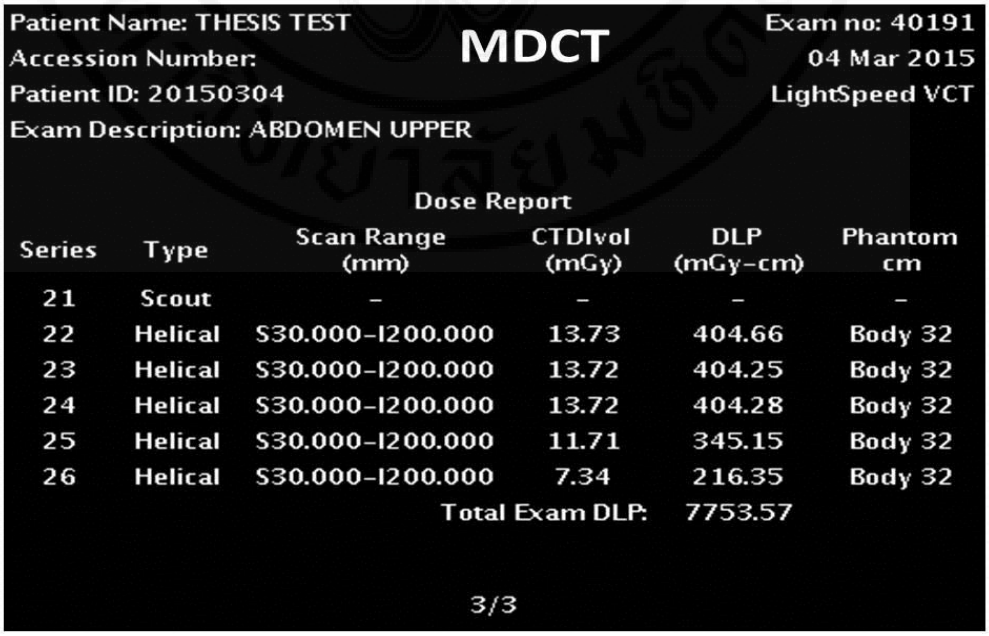

Patient Name: THESIS TEST
Accession Number:
Patient ID: 20150304
Exam Description: ABDOMEN UPPER

MDCT

Exam no: 40191
04 Mar 2015
LightSpeed VCT

Dose Report

Series	Type	Scan Range (mm)	CTDIvol (mGy)	DLP (mGy-cm)	Phantom cm
21	Scout	-	-	-	-
22	Helical	S30.000-I200.000	13.73	404.66	Body 32
23	Helical	S30.000-I200.000	13.72	404.25	Body 32
24	Helical	S30.000-I200.000	13.72	404.28	Body 32
25	Helical	S30.000-I200.000	11.71	345.15	Body 32
26	Helical	S30.000-I200.000	7.34	216.35	Body 32
			Total Exam DLP:	7753.57	

3/3

Figure 5.48 (C) Console displayed CT dose index of volume ($CTDI_{vol}$) and dose-length product (DLP) for MDCT.

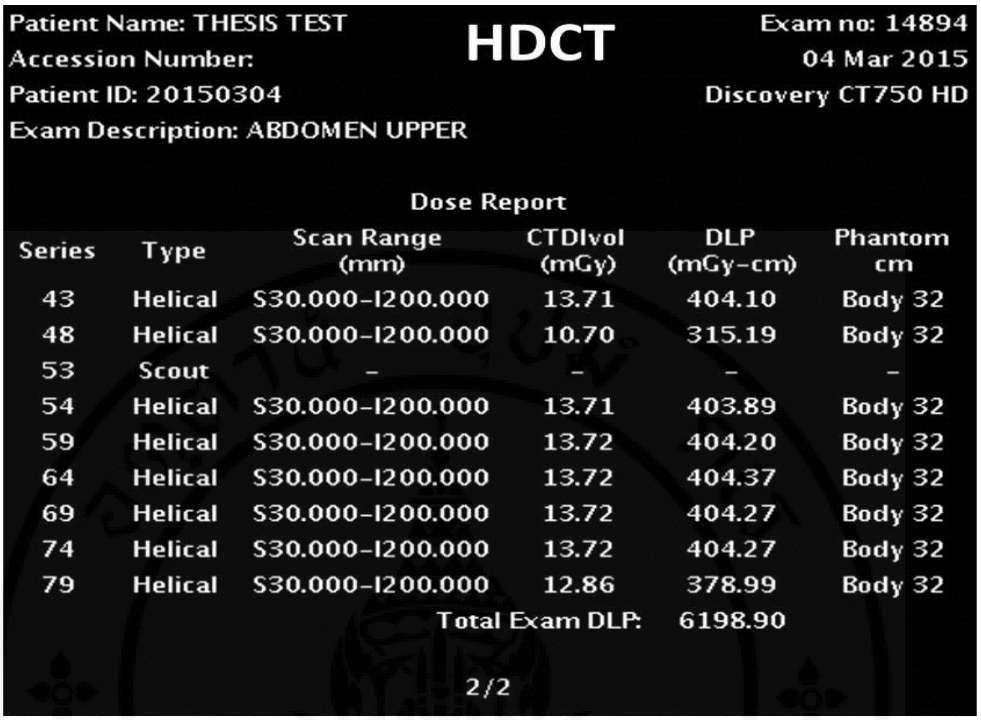

Patient Name: THESIS TEST
Accession Number:
Patient ID: 20150304
Exam Description: ABDOMEN UPPER

HDCT

Exam no: 14894
04 Mar 2015
Discovery CT750 HD

Dose Report

Series	Type	Scan Range (mm)	CTDIvol (mGy)	DLP (mGy-cm)	Phantom cm
43	Helical	S30.000-I200.000	13.71	404.10	Body 32
48	Helical	S30.000-I200.000	10.70	315.19	Body 32
53	Scout	-	-	-	-
54	Helical	S30.000-I200.000	13.71	403.89	Body 32
59	Helical	S30.000-I200.000	13.72	404.20	Body 32
64	Helical	S30.000-I200.000	13.72	404.37	Body 32
69	Helical	S30.000-I200.000	13.72	404.27	Body 32
74	Helical	S30.000-I200.000	13.72	404.27	Body 32
79	Helical	S30.000-I200.000	12.86	378.99	Body 32
			Total Exam DLP:	6198.90	

2/2

Figure 5.49 Console displayed CT dose index of volume ($CTDI_{vol}$) and dose-length product (DLP) for HDCT.

Table 5.13 Comparison of estimated effective dose between 2 scanners using all upper abdomen scan protocols at reference noise index from 0 to 20 for 3 sizes of phantoms.

Size	Noise index	Radiation dose (mSv)	
		MDCT	HDCT
Standard	0	6.86	6.88
	10	6.87	6.87
	15	6.6	5.87
	20	4.57	3.68
Large	0	6.87	6.88
	10	6.86	6.87
	15	6.82	6.61
	20	5.36	4.42
Very large	0	6.87	6.88
	10	6.87	6.88
	15	6.87	6.88
	20	6.44	5.21

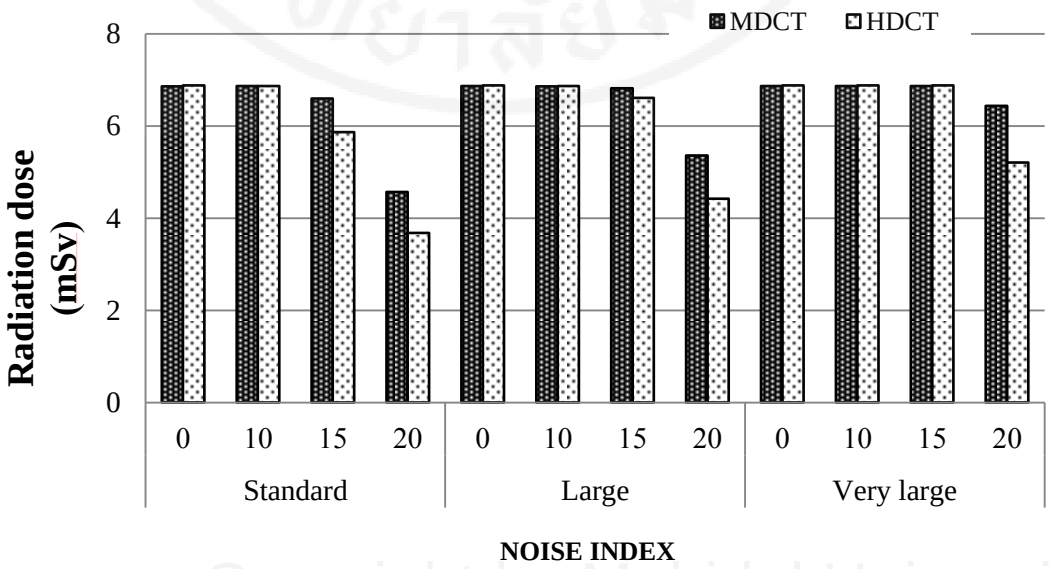

Figure 5.50 Estimated effective radiation dose (mSv) from 3 sizes of phantom at noise index from 0 to 20

Differences on estimated radiation doses using standard protocol for upper abdominal between MDCT and HDCT were minimal. HDCT dose was approximately 4 to 6% lower than MDCT.

The effect of phantom size on effective radiation doses was also minimal. Dose reduction was approximately 4% and 8% when increasing phantom size from standard to large and very large size in MDCT; 8% and 10% in HDCT respectively.

At reference noise index between 10 and 15, standard and large phantom size gave consistent patterns of estimated radiation dose, they were comparable for both MDCT and HDCT, 5.87 to 6.88 mSv for standard phantom size; 6.61 to 6.88 for large phantom size. At reference noise index 20, estimated effective dose from MDCT and HDCT was remarkable low, 4.57 mSv and 3.68 mSv for standard phantom size, 5.36 mSv and 4.42 mSv for large phantom size, but not for very large phantom size, the effective dose was comparable to those at reference noise index 10 and 15.

Body size-adapted CT protocol is a fundamental requirement for CT dose optimization to obtain the minimal radiation dose for acceptable diagnostic image quality.

CHAPTER VI
CONCLUSION

Experimental measurements in phantom study showed that measured noise index in all selected tissue ROIs decrease with the increase of slice thickness. At constant baseline noise index, the measured noise index averaged from selected tissue ROIs increased 22 to 29% as phantom size changed from standard to large and very large size. Increasing the noise index will result in a decreased radiation dose.

Differences on estimated radiation doses using standard protocol for upper abdominal between MDCT and HDCT were minimal. HDCT dose was approximately 4 to 6% lower than MDCT. The effect of phantom size on effective radiation doses was also minimal. Dose reduction was approximately 4 to 6% and 8 to 10 percent when increasing phantom size from standard to large and very large size respectively.

When the CT images in upper abdomen examination was acquired for improving image quality with filtered back-projection (FBP), adaptive statistical iterative reconstruction (ASIR) and model-based iterative reconstruction (MBIR) techniques, MBIR shows superior noise reduction than reconstructed with 30%ASIR, 40%ASIR and 50%ASIR and FBP. The reduced mage noise was 42, 37 and 38% lower than FBP for standard, large and very large size phantom respectively. The effect of phantom size on noise reduction was comparable for FBP and ASIR methods, but greater in MBIR.

The increase in radiation exposure due to CT scans has been of growing concern in recent years. Body size-adapted CT protocol is a fundamental part of CT dose optimization because the minimal radiation dose is required for diagnostic image quality in order to maximize the benefit-to-risk ratio of this imaging method.

REFERENCES

1. Kalra K M, MDCT Radiation Dose, In: Sanjay S, Rubin D G, Kalra K M,editor. MDCT A Practical Approach. Milan: Springer; 2006. P30-35

2. Understanding MEDICAL RADIATION. Computed Tomography (CT), Available from: http://www.medicalradiation.com/types-of-medical-imaging-using-x-rays/computed-tomography-ct. Retrieved April 27, 2017.

3.Yu L, Liu X, Leng S, Kofler JM, Ramirez-Giraldo JC, Qu M, et al. Radiation dose redution in computed tomography: techniques and future perspective. PMC 2012. Available from: http://www.ncbi.nlm.nih.gov/pmc/articles/ PMC3271708/ Retrieved April 20, 2017.

4. Madan R, Mannudeep K, Cynthia M, Hans DN. ICRP International System of Radiological Protection. Managing Patient Dose in Multi-Detector Computed Tomography (MDCT). Available from:http://www.icrp.org/ docs/ICRP-MDCT-for_web_ cons_32_219_06.pdf Retrieved April 20, 2017.

5. Pei-Jan PL, Thomas JB, Caridad B, Gerald C, Robert AJ, Robert JK, et al. Specification and Aceptance Testing of Computed Tomography Scanners. AAPM 1993. Available from: http://www.aapm.org/pubs/ reports / rpt_39.pdf Retrieved May 25, 2017.

6. Yu L, Liu X, Leng S, Kofler JM, Ramirez-Giraldo JC, Qu M, et al. Radiation Dose reduction in Computed Tomography: techniques and future perspective. PMC 2012. Available from: http://www.ncbi.nlm.nih.gov/pmc/articles/ PMC3271708/ Retrieved April 20, 2017.

7. Brink, JA, et al. "Helical CT: principles and technical considerations."Radiographics 1994 14(4):887. Available from: http://xrayphysics.com/ctsim.html Retrieved May 25, 2017.

8. Brink, JA, et al. "Helical CT: principles and technical considerations." Radiographics 1994 14(4):887. Available from: http://xrayphysics.com/ ctsim.html Retrieved May 25, 2017.

9. McNitt-Gray MF. Tradeoffs in CT Image Quality and Radiation Dose.AAPM 2006. Available from: http://www.aapm.org/meetings/04AM/pdf/14-2328-89141.pdf Retrieved April 20, 2017.

10. Sandra SH, Suhny A, Marcus YC, Ralph G, Mahadevappa M, Gilbert LR, et al. SCCT guidelines on radiation dose and dose-optimization strategies in cardiovascular CT. PMC 2012. Available from: https://www.ncbi.nlm.nih.gov/pmc/articles/ PMC3391026 Retrieved May 25, 2017.

11. Hairil R, Said M, Said R, Wan M. Effects of different tube potentials and iodine concentrations on image enhancement, contrast-to-noise ratio and noise in micro-CT images: a phantom study. Quant Imaging Med Surg. 2013 Oct; 3(5): 256–261. Available from: https://www.ncbi.nlm.nih.gov/pmc/articles/ PMC3834201 Retrieved April 20, 2017.

12. Nievelstein RA, van Dam IM, van der Molen AJ. Multidetector CT in children: current concepts and dose reduction strategies. PMC 2010 Aug; 40(8): 1324–1344. Available from: https://www.ncbi.nlm.nih.gov/pmc/articles/ PMC2895901 Retrieved April 20, 2017.

13. Pawana Inthibal. OPTIMIZATION IN 64-MDCT OF THE CHEST USING TUBE CURRENT MODULATION BASED ON NOISE INDEX: PHANTOM STUDY [Master of Science in the Program of Medical Imaging]. Bangkok Chulalongkorn Univesity, Thailand; 2012 Available from: http://thesis.grad.chula. ac.th/ cuthesis_form.php?loginid=5474 147630Retrieved April 20, 2017.

14. Angielina Protik . OPTIMIZATION OF IMAGE QUALITY IN PAEDIATRIC COMPUTED TOMOGRAPHY [Master of Science in the Program of Biomedical Physics]. Canada: Ryerson University; 2012. Available from: http://digital.library. ryerson.ca/islandora/object/RULA:979/datastream/ OBJ/ view Retrieved April 20, 2017.

15. Ehman EC, Yu L, ManducaA, Hara AK Fletsher JG. Methods forClinical Evaluation of Noise Reduction Methods at Computed Tomography. Available from: https://www.researchgate.net/scientific-contributions/442 25654_Eric_C_ Ehman Retrieved April 20, 2017.

16. Nuntue C, Krisanachinda A, Khamwan. Optimization of a low-dose 320-slice multi-detector computed tomography chest protocol using a phantom. Available from: https://www.researchgate.net/profile/Anchali_Krisana chinda2 Retrieved April 20, 2017.

17. Christner JA, Kofler JM, McCollough CH. Estimating effective dose for CT using dose-length product compared with using organ doses: consequences of adopting International Commission on Radiological Protection publication 103 or dual-energy scanning. AJR Am J Roentgenol. 2010;194 (4):881–9. [PubMed]

18. Huda W, Ogden KM, Khorasani MR.Conveerting Dose-Length Product to Effective Dose at CT. Radiology 2008 Available from: https://www.ncbi.nlm.nih.gov/pmc/articles/PMC2657852//Retrieved April 20, 2017.

19. Kobayashi M, Asada Y, Matsubara K, Haba T, Matsunaga Y, Kawaguchi A,et al. Evaluation of Effective Dose Using the k-Factor of optimal scan Range for CT Examination. Open Journal of Radiology 2015 Available from: https://file.scirp.org/pdf/OJRad2015090114414033.pdf Retrieved April 20, 2017.

20. Huda W, Ogden KM, KhorasaniMR. Converting Dose-Length Product to Effective Dose at CT. Radiology 2008 Available from: https://www.ncbi. nlm.nih.gov/pmc/articles/PMC2657852// Retrieved April 20, 2017.

BIOGRAPHY

NAME	Miss Saimai Siangyai
DATE OF BIRTH	11 October 1974
PLACE OF BIRTH	PRACHUAP KHIRI KHAN,THAILAND
INSTITUTIONS ATTENDED	Ramkhamhaeng University,2002-2004 Bachelor of Science (Radiological Science) Mahidol University,2013-2017 Master of Science (Radiological Science)
HOME ADDRESS	39/34 M.1Thawiwatthana, Bangkok 10170 Tel. 0819015044 E-mail: saimai_lovely@hotmail.com
EMPLOYMENT ADDRESS	Faculty of Medicine Vajira Hospital Navamindradhiraj University Tel. 022443244 E-mail: saimai@nmu.ac.th